Cell Reports
Medicine

Report

Anti-diabetic effects of GLP1 analogs are mediated by thermogenic interleukin-6 signaling in adipocytes

Graphical abstract

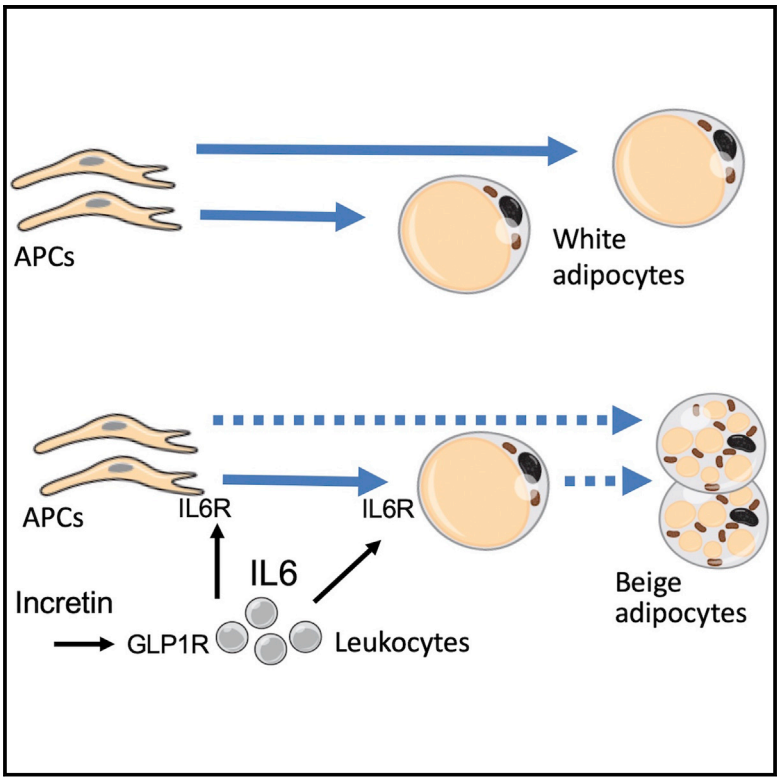

Highlights

- GLP1 signaling in monocytes leads to transient increase in circulating IL-6 levels
- IL-6 signaling in preadipocytes activates brown adipogenesis and thermogenesis
- IL-6 blockade suppresses liraglutide-induced anti-diabetic effects
- IL-6 signaling in adipocytes mediates liraglutide-induced anti-diabetic effects

Authors

Absalon D. Gutierrez, Zhanguo Gao, Vala Hamidi, ..., Hernan Vasquez, Heinrich Taegtmeyer, Mikhail G. Kolonin

Correspondence

absalon.d.gutierrez@uth.tmc.edu (A.D.G.), mikhail.g.kolonin@uth.tmc.edu (M.G.K.)

In brief

Anti-diabetic effects of incretins are mediated by multiple organs, and their effect on adipose tissue has remained unclear. Gutierrez et al. discover that GLP1 analogs induce IL-6 secretion by monocytes and show that IL-6 signaling in adipocytes activates brown adipogenesis and thermogenesis that contributes to anti-diabetic effects of GLP1 analogs.

Gutierrez et al., 2022, Cell Reports Medicine *3*, 100813
November 15, 2022
https://doi.org/10.1016/j.xcrm.2022.100813

CellPress

Cell Reports Medicine

CellPress
OPEN ACCESS

Report

Anti-diabetic effects of GLP1 analogs are mediated by thermogenic interleukin-6 signaling in adipocytes

Absalon D. Gutierrez,[1,*] Zhanguo Gao,[2] Vala Hamidi,[3] Liang Zhu,[4] Karla Bermudez Saint Andre,[5] Kayla Riggs,[6] Monika Ruscheinsky,[7] Hongyu Wang,[2] Yongmei Yu,[2] Charles Miller III,[8] Hernan Vasquez,[9] Heinrich Taegtmeyer,[9] and Mikhail G. Kolonin[2,10,*]

[1]Department of Internal Medicine, Division of Endocrinology, Diabetes and Metabolism, The University of Texas Health Science Center, Houston, TX 77030, USA
[2]The Brown Foundation Institute of Molecular Medicine, The University of Texas Health Science Center, Houston, TX 77030, USA
[3]Department of Medicine, Division of Endocrinology, University of California San Diego, La Jolla, CA 92093, USA
[4]Department of Internal Medicine, Division of Clinical and Translational Sciences, The University of Texas Health Science Center, Houston, TX 77030, USA
[5]Department of Medicine, Division of Endocrinology, Houston Methodist, Houston, TX 77030, USA
[6]Department of Internal Medicine, Division of Cardiology, University of Texas Southwestern, Dallas, TX 75225, USA
[7]Department of Pathology, University of Texas Southwestern, Dallas, TX 75390, USA
[8]Department of Cardiothoracic and Vascular Surgery, The University of Texas Health Science Center, Houston, TX 77030, USA
[9]Department of Internal Medicine, Division of Cardiovascular Medicine, The University of Texas Health Science Center, Houston, TX 77030, USA
[10]Lead contact
*Correspondence: absalon.d.gutierrez@uth.tmc.edu (A.D.G.), mikhail.g.kolonin@uth.tmc.edu (M.G.K.)
https://doi.org/10.1016/j.xcrm.2022.100813

SUMMARY

Mechanisms underlying anti-diabetic effects of GLP1 analogs remain incompletely understood. We observed that in prediabetic humans exenatide treatment acutely induces interleukin-6 (IL-6) secretion by monocytes and IL-6 in systemic circulation. We hypothesized that GLP1 analogs signal through IL-6 in adipose tissue (AT) and used the mouse model to test if IL-6 receptor (IL-6R) signaling underlies the effects of the GLP1-IL-6 axis. We show that liraglutide transiently increases IL-6 in mouse circulation and IL-6R signaling in AT. Metronomic liraglutide treatment resulted in AT browning and thermogenesis linked with STAT3 activation. IL-6-blocking antibody treatment inhibited STAT3 activation in AT and suppressed liraglutide-induced increase in thermogenesis and glucose utilization. We show that adipose IL-6R knockout mice still display liraglutide-induced weight loss but lack thermogenic adipocyte browning and metabolism activation. We conclude that the anti-diabetic effects of GLP1 analogs are mediated by transient upregulation of IL-6, which activates canonical IL-6R signaling and thermogenesis.

INTRODUCTION

Type 2 diabetes mellitus (T2DM) is a metabolic disease characterized by increased blood glucose, insulin resistance, and dyslipidemia.[1] T2DM development is linked with obesity, a condition of white adipose tissue (AT) overgrowth.[2] Dysfunction of adipocytes in visceral AT (VAT), resulting in chronic low-grade inflammation, is one of the pathogenic drivers.[3] Subcutaneous AT (SAT) on the other hand can protect from the metabolic syndrome through activation of mitochondria-rich adipocytes specialized to burn lipids through adaptive thermogenesis induced by sympathetic nervous system (SNS) stimuli directed by the hypothalamus.[4] The organ specialized in executing non-shivering thermogenesis is brown adipose tissue (BAT), which has fixed anatomic locations.[5] The "inducible/recruitable" brown-like (beige aka brite) adipocytes, arising in SAT in response to catecholamines activating adrenergic receptors, are functionally similar to adipocytes in the canonical (constitutive) BAT.[4] Brown and beige adipocytes enable thermogenic energy dissipation, which relies on the function of UCP1, a protein leaking protons to uncouple substrate oxidation from ATP synthesis.[5] Both BAT and beige adipocytes, when activated, dramatically increase the expenditure of both glucose and fatty acids, hence counteracting the metabolic consequences of obesity.[6,7]

Incretins are peptide hormones post-prandially secreted in the gut to lower blood glucose. Glucagon-like peptide-1 (GLP1) is an incretin signaling through the receptor GLP1R in various cell types.[8] Anti-diabetic effects of GLP1 and its analogs have been attributed to pancreatic GLP1R signaling activating insulin production.[9] A number of GLP1 mimetics, including liraglutide, exenatide, and dulaglutide, have been developed for

metronomic administration and sustained release in patients.[9,10] Incretin mimetics also have anti-obesity effects that are not completely understood.[8] AT mass control has been attributed in part to the effects of GLP1 analogs on the central nervous system (CNS) and appetite suppression.[11] However, the effects of GLP1 analogs in other organs, including the immune system, have been proposed to contribute to their efficacy.[12] Specifically, there is evidence for GLP1R expression and signaling in monocytes/macrophages.[13] Thermogenic AT activation by prolonged GLP1 analog treatment has been reported for both mice[14] and humans.[15]

Obesity is a chronic low-grade inflammatory state, and AT dysfunction is associated with leukocyte infiltration in AT and increased signaling via cytokines such as interleukin-6 (IL-6).[16] Interestingly, IL-6 signaling has context-specific effects and can be anti-diabetic.[17] The evolving paradigm shift is that, while chronic inflammation underlies T2DM, transient low-level inflammation stimulates beige adipogenesis, and hence may be beneficial.[18] The nuances of chronic versus acute IL-6 signaling are not well understood. IL-6 is secreted by leukocytes as well as other cell types,[19] and the IL-6 receptor (IL-6R) is expressed in numerous tissues, including AT.[20] IL-6 signals via IL-6R in cells expressing transmembrane IL-6R (canonical signaling) or *trans*-signaling via soluble IL-6R (sIL-6R) bound to ubiquitously expressed gp130 co-receptor.[19] In AT, IL-6 may act in autocrine/paracrine manner to influence insulin sensitivity through a number of mechanisms, including activation of AMP-activated protein kinase (AMPK).[21] IL-6 also acts as a Th2 cytokine stimulating AT macrophage proliferation and (alternative) M2 macrophage activation and hyperplasia, which indirectly affects AT physiology.[22] It has been shown that signaling of IL-6 family cytokines directs preadipocytes toward beige adipogenesis via signal transducer and activator of transcription 3 (STAT3).[18,23] Specifically, IL-6 directly activates IL-6R in adipocytes[24] and is required for normal activation of thermogenesis in AT.[25]

Here, based on the observation that IL-6 secretion by monocytes and that its systemic circulation is activated by GLP1 analogs in humans, we hypothesized that the GLP1-IL-6 axis induces adipose tissue browning. To test this, we used blocking IL-6 antibodies, as well as mice with IL-6R knockout (KO) in adipocyte progenitor cells (APCs) and in adipocytes. We show that adipose IL-6R KO mice lack thermogenic adipocyte browning and energy expenditure increase in response to liraglutide treatment. We conclude that the anti-diabetic effects of metronomically administered GLP1 analogs are mediated by transient upregulation of IL-6, which activates canonical IL-6R signaling and thermogenesis in adipocytes.

RESULTS

In humans, GLP1 signaling elevates circulating IL-6 activating STAT3 in preadipocytes

To investigate the systemic effects of GLP1 analogs, we analyzed the plasma of obese prediabetic patients enrolled in a prospective randomized crossover placebo-controlled double-blinded trial (NCT02104739) (Figure S1A) reported previously.[26] Participants were predominantly obese prediabetic males and females (Table S1). Acute changes in postprandial inflammatory and metabolic plasma markers were analyzed 2 h after exenatide or placebo administration. While circulating levels of insulin and free fatty acids (FFA) are known to be reduced by prolonged treatment with GLP1 analogs, neither insulin nor FFA was substantially affected by exenatide at the 2 h time point (Figures 1A and S1B). Changes in insulin and FFA circulation were observed only for the placebo arm, due to gastric emptying, which was also observed in previous studies.[27,28] Consistent with previous reports,[29] glucose only slightly decreased 2 h after exenatide while it increased after placebo (Figures 1A and S1B). Interestingly, IL-6 levels increased significantly from baseline to the 2-h time point (post-treatment) for exenatide ($p = 0.009$), but not for placebo ($p = 0.278$) (Figures 1A and S1B).

Macrophages and other myeloid cells are a major source of IL-6.[19] To test if they secrete IL-6 in response to GLP1 analogs, we used monocytes isolated based on adherence to plastic from peripheral blood mononuclear cells (PBMCs) of a healthy donor. After treatment with liraglutide at a concentration previously shown to activate GLP1R in cell culture,[30] IL-6 concentration was analyzed in medium 12 h later. Liraglutide induced a statistically significant rise in IL-6 secretion ($p < 0.001$), comparable to induction by lipopolysaccharide (LPS) used as a control IL-6 inducer (Figure 1B). In mouse models, prolonged GLP1 analog treatment has been reported to induce AT browning.[11,14] IL-6 family cytokines have also been reported to induce AT browning through STAT3 signaling in mouse models.[23,31] To investigate the potential effects of IL-6 on adipogenesis, we treated human preadipocytes with IL-6 (20 ng/mL). Western blotting with antibodies against phosphorylated STAT3 (Y705-pSTAT3), an IL-6 signaling marker, demonstrated its progressive induction over 30 to 120 min (Figure 1C). These results suggested that IL-6, induced by GLP1 analogs, signals on human preadipocytes and could mediate the metabolic response to incretin therapy.

Liraglutide-induced IL-6 signaling and adipocyte browning in mice

Next, we proceeded to test if GLP1 analog-induced AT browning is mediated by IL-6 signaling or if these processes are independent. To test if GLP1 analogs signal on adipocytes directly, we treated immortalized mouse pre-adipocytes cultured in brown adipogenesis medium with IL-6 (500 pg/mL) and/or liraglutide (100 nM) for 24 h. Western blotting demonstrated that IL-6, but not liraglutide alone, induces UCP1 expression (Figure 2A). These data, consistent with the lack of GLP1R expression in adipocytes,[8] indicate that IL-6 mediates the stimulatory effects of GLP1 analogs on brown adipogenesis and adaptive thermogenesis in AT.

To establish mice as a model to study the GLP1-IL-6 signaling axis, we challenged prediabetic overweight C57/B6 females ($n = 3$) with a single subcutaneous (s.c.) dose of liraglutide (400 μg/kg body weight [BW]). Plasma IL-6 levels were measured at 2, 6, and 24 h after liraglutide administration. An increase in circulating IL-6 was seen at 2 to 6 h ($p < 0.0001$) after liraglutide treatment (Figure 2B), followed by its subsequent clearance within 24 h. This indicated that the transient GLP1-IL-6 signaling axis is conserved in mice. Thermogenesis in brown adipocytes is linked with activation of lipolysis, which is expected to result in

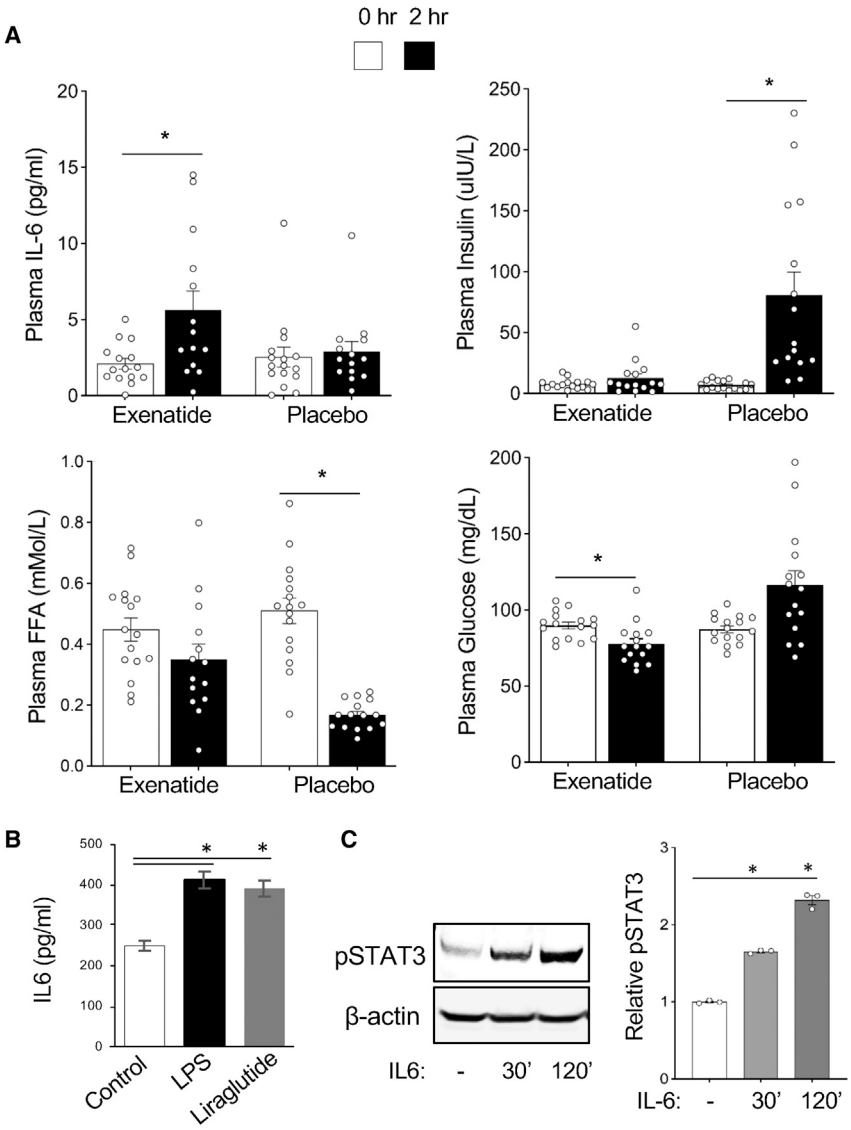

Figure 1. GLP1 signaling elevates circulating IL-6 activating STAT3 in preadipocytes

(A) Postprandial effects of exenatide. Baseline plasma was collected, immediately followed by subcutaneous injection of exenatide or placebo, immediately followed by a meal. Plasma was collected again 2 h after baseline collection. IL-6, insulin, FFA, and glucose levels were measured at both time points. *$p < 0.01$ (Student's t test); n = 16. Shown are mean values ± SEM.

(B) Liraglutide induces IL-6 secretion by human leukocytes. Human PBMCs were seeded at 2×10^6 cells/0.2 mL/well of RPMI 1640 containing 10% fetal bovine serum (FBS) onto a 48-well plate. After 24 h, medium and non-adherent cells were removed. Adherent monocytes were washed and treated with 200 μL RPMI 1640 medium containing 100 ng/mL of LPS or 100 nM liraglutide for 12 h. The supernatants were collected and IL-6 was measured. Shown are mean values ± SEM. **$p < 0.001$, Student's t test.

(C) Human SAT preadipocytes were seeded at 5×10^5 cells/well of 10% FBS DMEM medium onto a 12-well plate. After 24 h, medium was removed, and the cells were washed with PBS and maintained in 1% FBS DMEM overnight. Cells were then treated with 20 ng/mL of human IL-6, collected at the indicated time points, and subjected to immunoblotting with the indicated antibodies. Graph: quantification of band intensity normalized to actin. *$p < 0.001$, Student's t test.

reduced adiposity.[4] To assess the long-term effect of GLP1-IL-6 signaling, we used male mice fed high fat diet (HFD, 58%) from 4 weeks to 13 weeks of age. After 20 metronomic injections of 0.2 mg/kg liraglutide performed for 4 weeks, treated mice displayed reduced body weight increase, compared with vehicle-injected control mice (Figure S2A). This was due to reduced fat mass, as measured by Echo magnetic resonance imaging (MRI) performed before and after treatment (Figure 2C). We used the cold tolerance test (CTT) to measure thermogenesis, an indicator of brown adipocyte activity.[32] Compared with control mice, liraglutide-treated mice sustained higher core body temperatures, indicating brown adipocyte activation (Figure 2D). This was confirmed by analysis of tissue sections. Both VAT and SAT of liraglutide-treated mice contained smaller adipocytes (Figure 2E). Adipocytes in BAT of treated mice also had smaller lipid droplets (Figures 2E and S2B). Increased expression of UCP1 was detected by immunofluorescence (IF) in VAT and SAT, but not in BAT, of incretin-treated mice (Figures 2E and 2F). Increased VAT and SAT UCP1 expression was also confirmed by RT-PCR (Figure 2G) and western blotting (Figures 2H and S2C). Consistent with previous reports,[14,33] UCP1 induction was linked with increased AMPK phosphorylation, indicative of its activation (Figure 2H). As expected, UCP1 activation resulted in increased oxygen consumption of VAT and SAT, but not of BAT, as measured by Seahorse Mito Stress Assay (Figures S2D and S2E). The increase in AT respiration was also confirmed by Oroboros Oxygraph O2 k (Figure S2F).

Based on previous studies,[19] we used SOCS3 as a marker of canonical signaling and ADAM10 as a marker of *trans*-signaling to determine the mechanism of IL-6 function in AT. Both SOCS3 and ADAM10 were significantly increased in both SAT and VAT 30 min after liraglutide injection into mice (Figure 2I). This indicates that both IL-6R canonical and *trans*-signaling are activated by the liraglutide-IL-6 axis in AT. Notably, 24 h after IL-6 liraglutide both IL-6R canonical and *trans*-signaling returned to normal in males and were even lower in females injected with liraglutide (Figure S2G), consistent with a negative feedback loop reported previously.[34] Canonical and *trans* IL-6R signaling are mediated by STAT3 activation.[19] Western blotting on mouse AT extracts demonstrated that STAT3 and AMPK phosphorylation was increased at 30 to 120 min and decreased by 240 min after

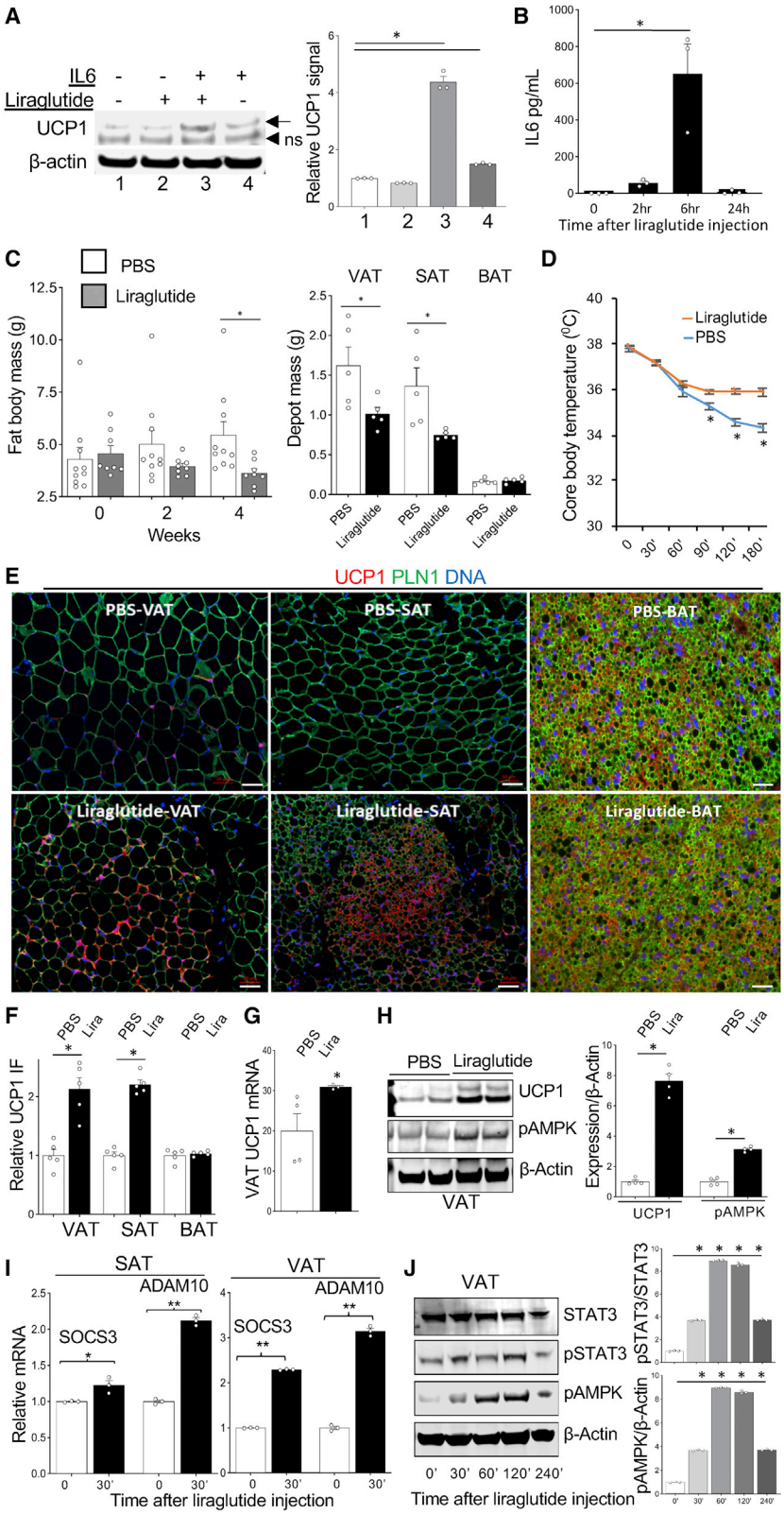

Figure 2. Liraglutide induces IL-6 signaling and adipocyte browning in mice

(A) Mouse immortalized brown pre-adipocytes seeded at confluency were induced for brown adipogenesis in DMEM/10% fetal bovine serum (FBS) medium containing 50 nM insulin/0.5 mM IBMX, 1 μM dexamethasone, 1 nM 3,5,3′-Triiodothyronine (T3), and 5 μM rosiglitazone for 24 h, were washed and cultured in DMEM/10% FBS medium containing 500 pg/mL mouse IL-6, 100 nM liraglutide, or their combination, for 6 and 24 h. UCP1 expression was measured by western blotting. Arrow: UCP1; ns, nonspecific band. Graph: quantification of band intensity normalized to actin. Shown are mean values ± SEM. *p < 0.001, one-way ANOVA.

(B) HFD-fed overweight C57BL/6 females (n = 3) were injected with a single s.c. dose of liraglutide (0.4 mg/kg BW). Plasma was collected at indicated time points after administration and IL-6 levels were measured by ELISA. Shown are mean values ± SEM. *p < 0.001, one-way ANOVA.

(C) Left: Echo MRI analysis of HFD-fed overweight C57BL/6 males after 2 and 4 weeks of liraglutide, treatment (0.2 mg/kg) shows a reduction of fat mass in liraglutide-treated mice. Right: mass of isolated individual AT depots at week 4. n = 5. *p = 0.05, Student's t test.

(D) Cold tolerance test in mice from experiment (C) at week 4. *p < 0.05, Student's t test.

(E) Analysis of SAT, VAT, and BAT sections from mice in (C) at week 4. Increased UCP1 expression is indicated (arrows). Adipocytes are revealed by perilipin-1 (PLN1) IF. Nuclei are blue. Scale bar, 50 μm.

(F) Quantification of data from (E). *p < 0.05, Student's t test.

(G) Analysis of VAT from mice in (C) at week 4 by RT-PCR showing relative UCP1 expression (normalized to 18S RNA) increased by liraglutide (Lira).

(H) Analysis of VAT from mice in (C) at week 4 by immunoblotting with the indicated antibodies in two mice per group (randomly selected) showing liraglutide-increased UCP1 and pAMPK signal.

(I) Nine-week-old C57BL/6 males were injected with a single s.c. dose of liraglutide (0.2 mg/kg BW). Analysis of SAT and VAT by RT-PCR after 30 min shows liraglutide-increased relative SOCS3 and ADAM10 expression (normalized to 18S RNA). *p < 0.05, **p < 0.01, Student's t test.

(J) C57BL/6 males were injected with a single s.c. dose of liraglutide (0.2 mg/kg BW). Analysis of VAT by immunoblotting shows liraglutide-induced pAMPK and pSTAT3 peaking at 120 min and decreasing at 240 min post-injection.

CellPress
OPEN ACCESS

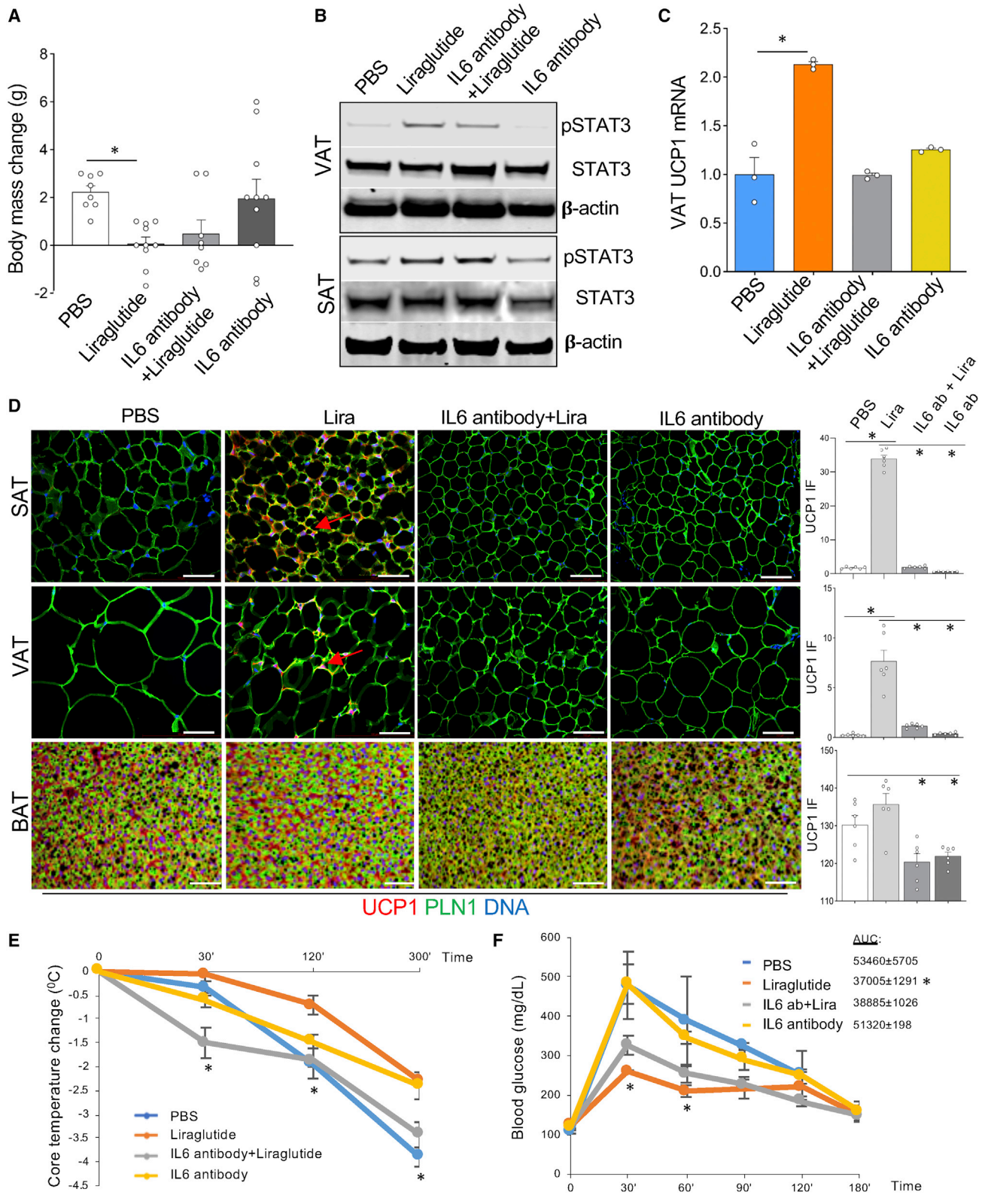

(legend on next page)

liraglutide injection (Figure 2J). This indicates that both canonical and *trans* IL-6R signaling are induced by the liraglutide-IL-6 axis transiently.

Liraglutide-induced AT beiging is suppressed by IL-6-blocking antibody

To investigate if GLP1 signaling effects on beige adipogenesis depend on the IL-6 pathway, we used a blocking anti-mouse IL-6 antibody. Male mice pre-fed HFD were treated with liraglutide alone, IL-6 antibody alone, or liraglutide/IL-6 antibody combination. Echo MRI was performed before and after treatment. After the 4-week injection course, liraglutide-treated mice had lower fat mass compared with vehicle-injected control mice (Figure 3A). Importantly, IL-6 antibody co-injection negated the effect of liraglutide on adiposity (Figure 3A). Western blotting on mouse AT extracted at the end of the experiment confirmed that STAT3 phosphorylation induced by liraglutide was partly blocked by IL-6 antibody (Figure 3B). As quantified by RT-PCR, UCP1 expression induction in AT by liraglutide was also blocked by IL-6 antibody (Figure 3C). The blockade of UCP1 induction by liraglutide was also confirmed by IF in both SAT and VAT of IL-6 antibody-treated mice (Figure 3D). CTT demonstrated that the ability to maintain higher core body temperature upon liraglutide treatment was significantly reduced by IL-6 antibody co-treatment (Figure 3E). Because GLP1 analogs have been shown to improve glucose homeostasis,[14] we also performed the glucose tolerance test (GTT). As expected, glucose control was significantly improved in the ''liraglutide alone'' group (Figure 3F). IL-6 antibody co-administration blunted the liraglutide effect on glucose tolerance. These data indicate that IL-6 signaling mediates liraglutide effects on adipocyte beiging, their thermogenic activity, and on glucose metabolism.

IL-6R knockout in adipocyte progenitors negates thermogenic effects of liraglutide

To test if GLP1 signaling-induced IL-6 promotes thermogenesis via direct canonical signaling in AT, we proceeded to knock out IL-6R in the adipocyte lineage. We and others have used lineage tracing to demonstrate that platelet-derived growth factor receptor beta (*Pdgfrb*) promoter marks APCs.[35] To create a model with a KO of IL-6R in APCs and their adipocyte derivatives, we used a previously reported approach[36] to cross *Pdgfrb*-Cre mice with IL-6R$^{fl/fl}$ mice, in which the IL-6R gene is flanked by loxP recombination sites. The resulting Pdgfrb-Cre; IL-6R$^{fl/fl}$ (KO) and control Cre-negative IL-6R$^{fl/fl}$ (WT) littermates were identified by PCR genotyping. IL-6R deletion was confirmed by IF on AT sections. As shown in Figure 4A, KO mice lack IL-6R specifically in Pdgfrβ+ adipose stroma but not in the endothelium. IL-6R KO was also confirmed by IF on SVF cells plated in culture (Figure S3A). Oxygen consumption measured by indirect calorimetry did not reveal changes in energy expenditure between WT and KO littermates (Figure S3B). Also, Echo MRI detected no difference in lean or fat body mass between WT and KO mice fed chow (Figure S3C). After HFD feeding for 1 month, both WT and KO mice gained more fat mass than chow-fed littermates, which was observed for both males and females (Figure S3C). HFD had no effect on lean or total body mass in either WT or APC-KO males or females (Figure S3C). These results show that IL-6R KO in APC does not have a significant effect on AT development.

To assess the response to GLP1 signaling activation, we used the same protocol as in Figure 2 to treat KO and WT mice with liraglutide. Echo MRI revealed that both male and female KO littermates had lower fat mass after liraglutide treatment, although weight loss extent did not reach statistical significance seen for WT mice (Figure 4B). This suggested that IL-6R in the adipocyte lineage may not directly mediate the weight loss effects of GLP1 analogs. However, while liraglutide-induced cold tolerance was observed in WT mice (Figure 2D), CTT 3 days after the last injection demonstrated that cold tolerance was not increased in KO males or females treated with liraglutide (Figure 4C). Analysis of adipose tissues did not detect a difference in adipocyte size between untreated WT and KO littermates for either VAT or SAT, consistent with their comparable fat mass. However, IF revealed that UCP1 expression induction by liraglutide was blunted in SAT and VAT of KO mice (Figure 4D). Baseline and liraglutide-induced UCP1 expression were also lower in BAT of KO mice compared with WT littermates (Figure 4D). The GTT revealed that glucose clearance increase by liraglutide, observed in WT mice, does not take place in KO littermates, which was the case for both males and females (Figure 4E). Moreover, the increase in energy expenditure in WT mice treated with liraglutide was not significant in KO littermates (Figure S3B). Finally, WT and KO mice displayed a trend for a different change in night-time respiratory exchange ratio (RER) upon liraglutide treatment (Figure 4F), although not statistically significant. Night-time RER tended to be lower in WT mice treated with liraglutide, suggesting increased lipid metabolism. In contrast, the night-time RER of liraglutide-treated KO mice was slightly higher, suggesting decreased lipid utilization for energy.

Figure 3. Liraglutide-induced AT beiging is suppressed by IL-6-blocking antibody

(A) Echo MRI analysis of HFD-fed overweight C57BL/6 males after 4 weeks of treatment with liraglutide (0.2 mg/kg), IL-6 antibody (5 mg/kg), or a combination of liraglutide and IL-6 antibody at doses above. Note that IL-6 antibody suppresses weight loss. *$p < 0.05$, one-way ANOVA.

(B) Analysis of VAT from mice in (A) at week 4 by immunoblotting with the indicated antibodies in randomly selected mice. Note that liraglutide-induced pSTAT3 is suppressed by IL-6 antibody.

(C) Analysis of VAT from mice in (A) at week 4 by RT-PCR shows that liraglutide-induced UCP1 expression (normalized to 18S RNA) is suppressed by IL-6 antibody. Shown is mean ± SEM, $n = 4$, *$p < 0.05$, one-way ANOVA.

(D) Analysis of SAT and VAT sections from mice in (A) at week 4. UCP1 expression (arrows) induced by liraglutide (Lira) is suppressed by IL-6 antibody. Adipocytes are revealed by perilipin-1 (PLN1) IF. Nuclei are blue. Scale bar, 50 μm. Graphs: the corresponding IF quantifications; *$p < 0.05$, one-way ANOVA.

(E) Analysis of mice in (A) at week 4 by cold tolerance test. Liraglutide-induced increase in body temperature maintenance (*$p < 0.05$ compared to PBS group, one-way ANOVA) is suppressed by IL-6 antibody. Plotted is core body temperature decrease from baseline (at 0 min at 4°C).

(F) Analysis of mice in (A) at week 4 by glucose tolerance test. Liraglutide-induced decrease in circulating glucose (*$p < 0.05$ compared to PBS group, one-way ANOVA) is suppressed by IL-6 antibody. AUC, area under the curve for each group.

We also tested if IL-6R in mature adipocytes is sufficient for mediating the effect of liraglutide on AT metabolism. Adiponectin-Cre and IL-6Ra$^{fl/fl}$ mice were crossed to generate Adiponectin-Cre; IL-6Ra$^{fl/fl}$ (adipo-KO) and control L6Ra$^{fl/fl}$ (WT) progeny. To assess the response to GLP1 signaling activation, we used the same protocol as in Figure 4 to treat adipo-KO and WT mice with liraglutide. Analysis of littermates demonstrated that adipo-KO mice had a phenotype similar to that of IL-6Ra KO in progenitor cells (Figure S4). In response to liraglutide, adipo-KO mice still lost fat mass (Figure S4A); however, did not display an improvement in glucose tolerance (Figure S4B), insulin sensitivity (Figure S4C), or cold tolerance (Figure S4D). Our data indicate that the canonical IL-6R signaling in adipocytes mediates liraglutide effects on thermogenic adipocyte activity, which modulates the systemic glucose/lipid metabolism balance.

DISCUSSION

Incretins have shown great promise in T2DM and obesity therapy. Here, based on the results of a prospective clinical trial, we report that acute GLP1 analog treatment induces IL-6 production by human monocytes and its increase in circulation. We corroborated these observations in mice and showed that metronomic treatment with a GLP1 analog liraglutide leads to thermogenic AT activation. Based on the notion that transient STAT3 activation, downstream of IL-6, can induce brown adipogenesis,[18] we hypothesized that the GLP1-IL-6 axis activates IL-6R signaling in adipocyte progenitors and/or adipocytes. We tested this hypothesis by performing IL-6 treatment and IL-6 blockade experiments and by inactivating IL-6R in the adipocyte lineage. We conclude that the direct effects of the transient GLP1-IL-6 axis activation in adipocytes modulate the systemic glucose/lipid metabolism balance.

Our study links GLP1 and IL-6 signaling with AT remodeling underlying the metabolic response. Previous studies in mouse models have revealed that both liraglutide[11,14] and IL-6[31] can induce AT browning. Our data, showing that liraglutide does not have a direct effect on adipocytes are consistent with adipocytes lacking GLP1R expression,[8] which suggests that the effects of GLP1 analogs are mediated by IL-6. Changes in AT in response to liraglutide have been attributed to their indirect effects on the hypothalamus mediated by the SNS,[11] and the resulting appetite inhibition, as well as to macrophage polarization.[37] Similarly, IL-6 has been reported to affect AT physiology indirectly via SNS and macrophage activation.[31,38] The anti-obesity effects of interaction between GLP1 and IL-6 signaling in the CNS have been established.[39] However, direct effect of either GLP1 analogs or of IL-6 on adipose cells, with implications for AT beiging and metabolism activation, has not been reported *in vivo*. The notion of the link between these two pathways has been limited to reports on IL-6 regulating endogenous GLP1 secretion[24,40] and controlling glycemic homeostasis by delaying gastric emptying.[41] Our findings uncover a novel link between GLP1 analogs and IL-6 through IL-6-IL-6R signaling induced downstream of GLP1R activation in monocytes. Our discovery is consistent with GLP1R signaling importance in macrophages reported recently.[13] The mechanism of monocyte IL-6 expression induction by GLP1 analogs remains to be established. Interestingly, nuclear factor kappa B (NfκB), a key activator of IL-6 expression, is suppressed by GLP1 analogs.[42] We speculate that signaling is mediated by cAMP-response element-binding protein (CREB) known to be downstream of GLP1R and activating IL-6 transcription.[43,44]

Our results are consistent with the previous study showing that transplantation of BAT into IL-6 KO mice fails to improve glucose homeostasis.[45] The mechanism through which IL-6 signaling activates adipocyte thermogenesis also remains to be fully elucidated. A recent study shows that adipocyte-derived IL-6 promotes insulin resistance and AT macrophage infiltration, while myeloid-derived IL-6 promoted beneficial metabolic effects.[19] However, STAT3, activated by both canonical and *trans* IL-6R signaling, appears to mediate the effects of IL-6, as previously reported.[46,47] Consistent with our findings, STAT3 activation has been implicated in GLP1-induced M2 macrophage polarization.[48] There is sufficient evidence that IL-6 acts on APCs and directs their differentiation toward brown adipogenesis.[18,23,49] Therefore, the loss of thermogenic response observed in IL-6R KO mice in our study is likely to be due, at least in part, to IL-6 signaling loss in preadipocytes. However, mature adipocyte *trans*-differentiation reported previously[4] could also partly account for the phenotype, as IL-6R is also missing in mature adipocytes in the Pdgfrb-Cre model. In fact, UCP1 expression induction in cultured adipocytes upon treatment has been reported.[50] AMPK, activated in AT by GLP1 signaling, is a possible mechanism mediating IL-6R signaling in adipocytes.[21,51]

AMPK activation downstream of IL-6 signaling has been implicated as an explanation for its effects on AT thermogenesis and metabolism.[31,34] AMPK plays an important role in mitochondrial biogenesis.[52] Consistent with this, thermogenesis in AT relies on AMPK activity.[53] IL-6 signaling is also known to induce lipolysis,[54] the process underlying incretin-induced weight loss. However, liraglutide induced weight loss irrespective of IL-6R expression in our study. This suggests that the anti-obesity effects of GLP1 signaling are at least in part uncoupled from thermogenic signaling activated by IL-6. In fact, AMPK is induced in adipocytes undergoing lipolysis to activate a negative feedback loop suppressing lipase activity.[55] Notably, pAMPK increase in response to liraglutide was observed irrespective of IL-6R in adipocytes (data not shown). The role of AMPK in mediating the effect of GLP1-IL-6 axis on adipocytes remains to be better understood. Because IL-6 also promotes myogenesis,[56] its potential anti-diabetic effects in skeletal muscle, a major site of glucose disposal, could contribute to its effects in mediating liraglutide signaling.

In summary, our study sheds new light on the role of GLP1 signaling on the immune system and AT metabolism and establishes a previously overlooked mechanism. This study has not tested whether gastric inhibitory polypeptide, another incretin signaling through a distinct receptor, also activates this pathway. The clinical contribution of AT thermogenesis activation by GLP1 analogs to their overall anti-diabetic effects in humans remains to be determined. There is a report suggesting that brown AT metabolism may be activated by GLP1 analogs in humans.[15]

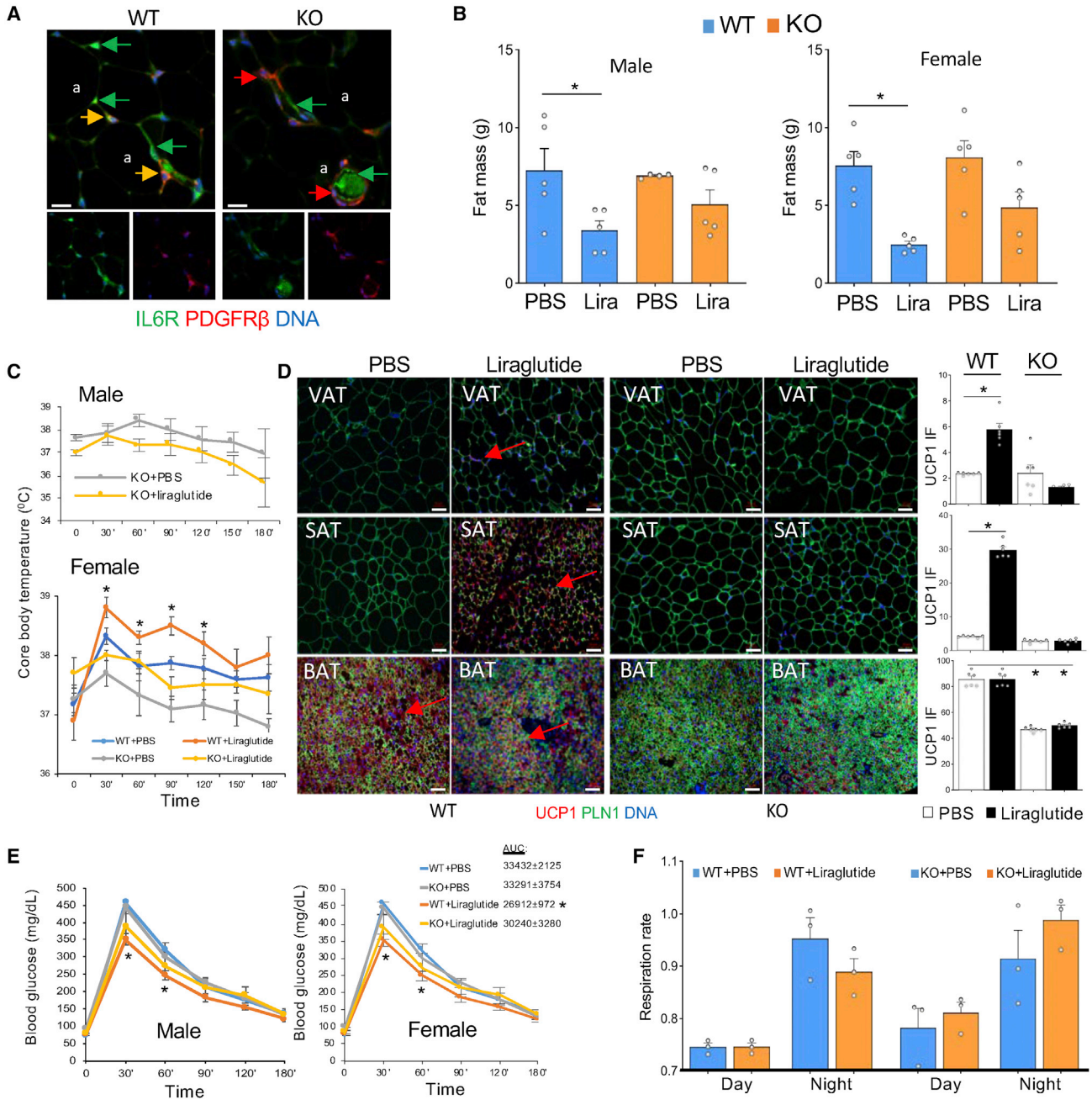

Figure 4. IL-6R KO in adipocyte progenitors negates the thermogenic effect of liraglutide

(A) Paraffin sections of AT from WT and Pdgfrb-Cre; IL-6R$^{fl/fl}$ (KO) mice subjected to IF. Note that IL-6R protein expression (green) in PDGFRβ-positive ASCs (red, resulting in yellow signal in WT mice) is lost in ASC but not in PDGFRβ-negative endothelium of KO mice. a, adipocytes. Scale bar, 50 μm.

(B) Echo MRI analysis of HFD-fed overweight C57BL/6 and KO males and females after 4 weeks of liraglutide, treatment. Note the reduction of fat mass in both WT and KO liraglutide-treated mice. n = 5. *p < 0.05, Student's t test.

(C) Cold tolerance test in mice from (B) at week 4. Note that liraglutide-induced improvement in body temperature maintenance is not observed in KO mice (*p < 0.05 for WT + PBS versus WT + Liraglutide, one-way ANOVA).

(D) Analysis of AT sections from mice in (B) at week 4. Note that liraglutide-induced UCP1 expression increase (arrows) is not observed in SAT and reduced in BAT of KO mice. Adipocytes are revealed by perilipin-1 (PLN1) IF. Nuclei are blue. Scale bar, 50 μm. Graphs: the corresponding IF quantifications; *p < 0.05, one-way ANOVA.

(E) Analysis of mice in (B) at week 4 by glucose tolerance test. Liraglutide-induced decrease in circulating glucose (*p < 0.05 compared with PBS group, one-way ANOVA) is reduced in KO mice. AUC, area under the curve for each female group.

(F) Respiratory exchange ratio (RER = VCO_2/VO_2) in mice from experiment in (B) at week 4. Average night and day plots show a significant decrease by liraglutide in WT mice, and an increase in KO mice.

Clinically, GLP1 analogs have been shown to affect a wide spectrum of pathways, including the production of apolipoprotein B[57] and fat-secreted ceramides,[58] the markers of cardiovascular disease. In light of recent clinical findings,[59] it will be important to investigate how this pathway contributes to the effect of exercise on healthy weight loss maintenance in patients treated with incretins. It also remains to be established whether IL-6 signaling mediates the anti-diabetic effects of GLP1 analogs in patients. As IL-6 antagonists have been considered for use in patients with metabolic disease,[60] the potential implications on GLP1 signaling response are important to consider.

Limitations of the study

The potential importance of BAT for mediating GLP1 analog effects remains to be further characterized. This issue may be particularly clinically relevant due to the differences in BAT abundance and function between mice and humans.

STAR★METHODS

Detailed methods are provided in the online version of this paper and include the following:

- KEY RESOURCES TABLE
- RESOURCE AVAILABILITY
  - Lead contact
  - Materials availability
  - Data and code availability
- EXPERIMENTAL MODEL AND SUBJECT DETAILS
  - Human subjects
  - Animals
- METHOD DETAILS
  - Cell analysis
  - Tissue analysis
  - Quantitative real-time RT-PCR
  - Western blotting
- QUANTIFICATION AND STATISTICAL ANALYSIS
- ADDITIONAL RESOURCES

SUPPLEMENTAL INFORMATION

Supplemental information can be found online at https://doi.org/10.1016/j.xcrm.2022.100813.

ACKNOWLEDGMENTS

We thank Kathy Franco, Theresa Danczak, Meagan Olivares, Kayla Ruch, Vu Ta, Christine Wong, Truong Lam, Sara Coverdale, Amy Dursteler, Hiba Ali, Nitya Kumar, MinJae Lee, the UT Houston Clinical Research Unit, Memorial Hermann Investigational Drug Services, Memorial Hermann Food and Nutrition Services, and Quest Laboratories for excellent clinical trial support and laboratory assistance. We thank Jon Tyson and Philip Orlander for assistance in protocol development and oversight. We thank Rebecca Berdeaux and Antonio Soares for help with Oroboros. This work was supported by grant R21DK122234 from the NIH as well as by the CCTS funded through NIH Award UL1 TR000371 and KL2 TR000370 from the National Center for Advancing Translational Research to A.D.G. M.G.K. is supported by the Bovay Foundation and by the Levy Fund. H.T. receives support from R01-HL-61483-15.

AUTHOR CONTRIBUTIONS

A.D.G. designed and oversaw the study, obtained funding, interpreted the data, and edited the manuscript. M.G.K. designed experiments, analyzed data, and wrote the manuscript. H.T. contributed to protocol development and oversight. Z.G. and Y.Y. performed experiments and collected and interpreted data. V.H. revised the manuscript, assisted with experiments, and contributed to data collection and interpretation. L.Z. conducted the statistical analyses and revised the manuscript. K.B.S.M., M.R., and K.R. contributed to material and data collection/interpretation and manuscript preparation. H.V. performed western blots and provided manuscript assistance. H.W. contributed to data collection and interpretation. C.M. assisted with protocol development and statistical analyses. A.D.G. is the guarantor of this work and, as such, has full access to all the study data and takes responsibility for the integrity of the data and the accuracy of the data analysis.

DECLARATION OF INTERESTS

A.D.G. previously served on the Speakers' Bureau for AstraZeneca Pharmaceuticals. AstraZeneca provided study medications for the randomized controlled trial but was not involved in study design, data analyses, or manuscript preparation.

Received: March 3, 2022
Revised: September 6, 2022
Accepted: October 17, 2022
Published: November 15, 2022

REFERENCES

1. Roden, M., and Shulman, G.I. (2019). The integrative biology of type 2 diabetes. Nature *576*, 51–60.
2. Blüher, M. (2019). Obesity: global epidemiology and pathogenesis. Nat. Rev. Endocrinol. *15*, 288–298.
3. Ghaben, A.L., and Scherer, P.E. (2019). Adipogenesis and metabolic health. Nat. Rev. Mol. Cell Biol. *20*, 242–258.
4. Kajimura, S., Spiegelman, B.M., and Seale, P. (2015). Brown and beige fat: physiological roles beyond heat generation. Cell Metabol. *22*, 546–559.
5. Nedergaard, J., and Cannon, B. (2014). The browning of white adipose tissue: some burning issues. Cell Metabol. *20*, 396–407.
6. Almind, K., Manieri, M., Sivitz, W.I., Cinti, S., and Kahn, C.R. (2007). Ectopic brown adipose tissue in muscle provides a mechanism for differences in risk of metabolic syndrome in mice. Proc. Natl. Acad. Sci. USA *104*, 2366–2371.
7. Lowell, B.B., S-Susulic, V., Hamann, A., Lawitts, J.A., Himms-Hagen, J., Boyer, B.B., Kozak, L.P., and Flier, J.S. (1993). Development of obesity in transgenic mice after genetic ablation of brown adipose tissue. Nature *366*, 740–742.
8. Drucker, D.J. (2018). The ascending GLP-1 road from clinical safety to reduction of cardiovascular complications. Diabetes *67*, 1710–1719.
9. Müller, T.D., Finan, B., Bloom, S.R., D'Alessio, D., Drucker, D.J., Flatt, P.R., Fritsche, A., Gribble, F., Grill, H.J., Habener, J.F., et al. (2019). Glucagon-like peptide 1 (GLP-1). Mol. Metabol. *30*, 72–130.
10. Knudsen, L.B., Nielsen, P.F., Huusfeldt, P.O., Johansen, N.L., Madsen, K., Pedersen, F.Z., Thøgersen, H., Wilken, M., and Agersø, H. (2000). Potent derivatives of glucagon-like peptide-1 with pharmacokinetic properties suitable for once daily administration. J. Med. Chem. *43*, 1664–1669.
11. Beiroa, D., Imbernon, M., Gallego, R., Senra, A., Herranz, D., Villarroya, F., Serrano, M., Fernø, J., Salvador, J., Escalada, J., et al. (2014). GLP-1 agonism stimulates brown adipose tissue thermogenesis and browning through hypothalamic AMPK. Diabetes *63*, 3346–3358.
12. Baggio, L.L., and Drucker, D.J. (2021). Glucagon-like peptide-1 receptor co-agonists for treating metabolic disease. Mol. Metabol. *46*, 101090.

13. Chen, J., Mei, A., Liu, X., Braunstein, Z., Wei, Y., Wang, B., Duan, L., Rao, X., Rajagopalan, S., Dong, L., and Zhong, J. (2022). Glucagon-like peptide-1 receptor regulates macrophage migration in monosodium urate-induced peritoneal inflammation. Front. Immunol. *13*, 876934.

14. Han, F., Hou, N., Liu, Y., Huang, N., Pan, R., Zhang, X., Mao, E., and Sun, X. (2019). Liraglutide improves vascular dysfunction by regulating a cAMP-independent PKA-AMPK pathway in perivascular adipose tissue in obese mice. Biomed. Pharmacother. *120*, 109537.

15. Janssen, L.G.M., Nahon, K.J., Bracké, K.F.M., van den Broek, D., Smit, R., Sardjoe Mishre, A.S.D., Koorneef, L.L., Martinez-Tellez, B., Burakiewicz, J., Kan, H.E., et al. (2020). Twelve weeks of exenatide treatment increases [(18)F]fluorodeoxyglucose uptake by brown adipose tissue without affecting oxidative resting energy expenditure in nondiabetic males. Metabolism: Clin. Metabolism *106*, 154167.

16. Ouchi, N., Parker, J.L., Lugus, J.J., and Walsh, K. (2011). Adipokines in inflammation and metabolic disease. Nat. Rev. Immunol. *11*, 85–97.

17. Mauer, J., Denson, J.L., and Brüning, J.C. (2015). Versatile functions for IL-6 in metabolism and cancer. Trends Immunol. *36*, 92–101.

18. Sun, K., Gao, Z., and Kolonin, M.G. (2018). Transient inflammatory signaling promotes beige adipogenesis. Sci. Signal. *11*, eaat3192.

19. Han, M.S., White, A., Perry, R.J., Camporez, J.P., Hidalgo, J., Shulman, G.I., and Davis, R.J. (2020). Regulation of adipose tissue inflammation by interleukin 6. Proc. Natl. Acad. Sci. USA *117*, 2751–2760.

20. Kraakman, M.J., Kammoun, H.L., Allen, T.L., Deswaerte, V., Henstridge, D.C., Estevez, E., Matthews, V.B., Neill, B., White, D.A., Murphy, A.J., et al. (2015). Blocking IL-6 trans-signaling prevents high-fat diet-induced adipose tissue macrophage recruitment but does not improve insulin resistance. Cell Metabol. *21*, 403–416.

21. Ruderman, N.B., Keller, C., Richard, A.M., Saha, A.K., Luo, Z., Xiang, X., Giralt, M., Ritov, V.B., Menshikova, E.V., Kelley, D.E., et al. (2006). Interleukin-6 regulation of AMP-activated protein kinase. Potential role in the systemic response to exercise and prevention of the metabolic syndrome. Diabetes *55*, S48–S54.

22. Braune, J., Weyer, U., Hobusch, C., Mauer, J., Brüning, J.C., Bechmann, I., and Gericke, M. (2017). IL-6 regulates M2 polarization and local proliferation of adipose tissue macrophages in obesity. J. Immunol. *198*, 2927–2934.

23. Babaei, R., Schuster, M., Meln, I., Lerch, S., Ghandour, R.A., Pisani, D.F., Bayindir-Buchhalter, I., Marx, J., Wu, S., Schoiswohl, G., et al. (2018). Jak-TGFbeta cross-talk links transient adipose tissue inflammation to beige adipogenesis. Sci. Signal. *11*, eaai7838.

24. Wueest, S., Laesser, C.I., Böni-Schnetzler, M., Item, F., Lucchini, F.C., Borsigova, M., Müller, W., Donath, M.Y., and Konrad, D. (2018). IL-6-Type cytokine signaling in adipocytes induces intestinal GLP-1 secretion. Diabetes *67*, 36–45.

25. Knudsen, J.G., Murholm, M., Carey, A.L., Biensø, R.S., Basse, A.L., Allen, T.L., Hidalgo, J., Kingwell, B.A., Febbraio, M.A., Hansen, J.B., and Pilegaard, H. (2014). Role of IL-6 in exercise training- and cold-induced UCP1 expression in subcutaneous white adipose tissue. PLoS One *9*, e84910.

26. Hamidi, V., Riggs, K., Zhu, L., Bermudez Saint Andre, K., Westby, C., Coverdale, S., Dursteler, A., Wang, H., Miller Iii, C., Taegtmeyer, H., and Gutierrez, A.D. (2020). Acute exenatide therapy attenuates postprandial vasodilation in humans with prediabetes: a randomized controlled trial. Metab. Syndr. Relat. Disord. *18*, 225–233.

27. DeFronzo, R.A., Okerson, T., Viswanathan, P., Guan, X., Holcombe, J.H., and MacConell, L. (2008). Effects of exenatide versus sitagliptin on postprandial glucose, insulin and glucagon secretion, gastric emptying, and caloric intake: a randomized, cross-over study. Curr. Med. Res. Opin. *24*, 2943–2952.

28. Gastaldelli, A., Gaggini, M., Daniele, G., Ciociaro, D., Cersosimo, E., Tripathy, D., Triplitt, C., Fox, P., Musi, N., DeFronzo, R., and Iozzo, P. (2016). Exenatide improves both hepatic and adipose tissue insulin resistance: a dynamic positron emission tomography study. Hepatology *64*, 2028–2037.

29. Schwartz, E.A., Koska, J., Mullin, M.P., Syoufi, I., Schwenke, D.C., and Reaven, P.D. (2010). Exenatide suppresses postprandial elevations in lipids and lipoproteins in individuals with impaired glucose tolerance and recent onset type 2 diabetes mellitus. Atherosclerosis *212*, 217–222.

30. Shi, L., Ji, Y., Jiang, X., Zhou, L., Xu, Y., Li, Y., Jiang, W., Meng, P., and Liu, X. (2015). Liraglutide attenuates high glucose-induced abnormal cell migration, proliferation, and apoptosis of vascular smooth muscle cells by activating the GLP-1 receptor, and inhibiting ERK1/2 and PI3K/Akt signaling pathways. Cardiovasc. Diabetol. *14*, 18.

31. Li, G., Klein, R.L., Matheny, M., King, M.A., Meyer, E.M., and Scarpace, P.J. (2002). Induction of uncoupling protein 1 by central interleukin-6 gene delivery is dependent on sympathetic innervation of brown adipose tissue and underlies one mechanism of body weight reduction in rats. Neuroscience *115*, 879–889.

32. Cannon, B., and Nedergaard, J. (2004). Brown adipose tissue: function and physiological significance. Physiol. Rev. *84*, 277–359.

33. Zhou, J., Poudel, A., Chandramani-Shivalingappa, P., Xu, B., Welchko, R., and Li, L. (2019). Liraglutide induces beige fat development and promotes mitochondrial function in diet induced obesity mice partially through AMPK-SIRT-1-PGC1-alpha cell signaling pathway. Endocrine *64*, 271–283.

34. L Sarvas, J., Khaper, N., and Lees, S.J. (2013). The IL-6 paradox: context dependent interplay of SOCS3 and AMPK. J. Diabetes Metabol. *01*.

35. Gao, Z., Daquinag, A.C., Su, F., Snyder, B., and Kolonin, M.G. (2018). PDGFRalpha/PDGFRbeta signaling balance modulates progenitor cell differentiation into white and beige adipocytes. Development *145*. dev155861-13.

36. Su, F., Daquinag, A.C., Ahn, S., Saha, A., Dai, Y., Zhao, Z., DiGiovanni, J., and Kolonin, M.G. (2021). Progression of prostate carcinoma is promoted by adipose stromal cell-secreted CXCL12 signaling in prostate epithelium. NPJ Precis. Oncol. *5*, 26. https://doi.org/10.1038/s41698-021-00160-9.

37. Zhuge, F., Ni, Y., Nagashimada, M., Nagata, N., Xu, L., Mukaida, N., Kaneko, S., and Ota, T. (2016). DPP-4 inhibition by linagliptin attenuates obesity-related inflammation and insulin resistance by regulating M1/M2 macrophage polarization. Diabetes *65*, 2966–2979.

38. Wueest, S., and Konrad, D. (2020). The controversial role of IL-6 in adipose tissue on obesity-induced dysregulation of glucose metabolism. Am. J. Physiol. Endocrinol. Metab. *319*, E607–E613.

39. Jansson, J.O., and Palsdottir, V. (2015). Brain IL-6–where amylin and GLP-1 antiobesity signaling congregate. Diabetes *64*, 1498–1499.

40. Ellingsgaard, H., Hauselmann, I., Schuler, B., Habib, A.M., Baggio, L.L., Meier, D.T., Eppler, E., Bouzakri, K., Wueest, S., Muller, Y.D., et al. (2011). Interleukin-6 enhances insulin secretion by increasing glucagon-like peptide-1 secretion from L cells and alpha cells. Nat. Med. *17*, 1481–1489.

41. Lang Lehrskov, L., Lyngbaek, M.P., Soederlund, L., Legaard, G.E., Ehses, J.A., Heywood, S.E., Wewer Albrechtsen, N.J., Holst, J.J., Karstoft, K., Pedersen, B.K., and Ellingsgaard, H. (2018). Interleukin-6 delays gastric emptying in humans with direct effects on glycemic control. Cell Metabol. *27*, 1201–1211.e3.

42. Krasner, N.M., Ido, Y., Ruderman, N.B., and Cacicedo, J.M. (2014). Glucagon-like peptide-1 (GLP-1) analog liraglutide inhibits endothelial cell inflammation through a calcium and AMPK dependent mechanism. PLoS One *9*, e97554.

43. Chava, K.R., Karpurapu, M., Wang, D., Bhanoori, M., Kundumani-Sridharan, V., Zhang, Q., Ichiki, T., Glasgow, W.C., and Rao, G.N. (2009). CREB-mediated IL-6 expression is required for 15(S)-hydroxyeicosatetraenoic acid-induced vascular smooth muscle cell migration. Arterioscler. Thromb. Vasc. Biol. *29*, 809–815.

44. Lee, J.H., Wen, X., Cho, H., and Koo, S.H. (2018). CREB/CRTC2 controls GLP-1-dependent regulation of glucose homeostasis. Faseb. J. *32*, 1566–1578.

45. Stanford, K.I., Middelbeek, R.J.W., Townsend, K.L., An, D., Nygaard, E.B., Hitchcox, K.M., Markan, K.R., Nakano, K., Hirshman, M.F., Tseng, Y.H., and Goodyear, L.J. (2013). Brown adipose tissue regulates glucose homeostasis and insulin sensitivity. J. Clin. Invest. *123*, 215–223.

46. Gliniak, C.M., and Scherer, P.E. (2019). Critical lipids link breastfeeding to healthy adipose tissue in infancy and adulthood. J. Clin. Invest. *129*, 2198–2200.

47. Derecka, M., Gornicka, A., Koralov, S.B., Szczepanek, K., Morgan, M., Raje, V., Sisler, J., Zhang, Q., Otero, D., Cichy, J., et al. (2012). Tyk2 and Stat3 regulate brown adipose tissue differentiation and obesity. Cell Metabol. *16*, 814–824.

48. Shiraishi, D., Fujiwara, Y., Komohara, Y., Mizuta, H., and Takeya, M. (2012). Glucagon-like peptide-1 (GLP-1) induces M2 polarization of human macrophages via STAT3 activation. Biochem. Biophys. Res. Commun. *425*, 304–308.

49. Kristóf, E., Klusóczki, Á., Veress, R., Shaw, A., Combi, Z.S., Varga, K., Győry, F., Balajthy, Z., Bai, P., Bacso, Z., and Fésüs, L. (2019). Interleukin-6 released from differentiating human beige adipocytes improves browning. Exp. Cell Res. *377*, 47–55.

50. Petruzzelli, M., Schweiger, M., Schreiber, R., Campos-Olivas, R., Tsoli, M., Allen, J., Swarbrick, M., Rose-John, S., Rincon, M., Robertson, G., et al. (2014). A switch from white to brown fat increases energy expenditure in cancer-associated cachexia. Cell Metabol. *20*, 433–447.

51. Chen, X.L., Wang, Y., Peng, W.W., Zheng, Y.J., Zhang, T.N., Wang, P.J., Huang, J.D., and Zeng, Q.Y. (2018). Effects of interleukin-6 and IL-6/AMPK signaling pathway on mitochondrial biogenesis and astrocytes viability under experimental septic condition. Int. Immunopharm. *59*, 287–294.

52. Jornayvaz, F.R., and Shulman, G.I. (2010). Regulation of mitochondrial biogenesis. Essays Biochem. *47*, 69–84.

53. Wu, L., Zhang, L., Li, B., Jiang, H., Duan, Y., Xie, Z., Shuai, L., Li, J., and Li, J. (2018). AMP-activated protein kinase (AMPK) regulates energy metabolism through modulating thermogenesis in adipose tissue. Front. Physiol. *9*, 122.

54. van Hall, G., Steensberg, A., Sacchetti, M., Fischer, C., Keller, C., Schjerling, P., Hiscock, N., Møller, K., Saltin, B., Febbraio, M.A., and Pedersen, B.K. (2003). Interleukin-6 stimulates lipolysis and fat oxidation in humans. J. Clin. Endocrinol. Metab. *88*, 3005–3010.

55. Kim, S.J., Tang, T., Abbott, M., Viscarra, J.A., Wang, Y., and Sul, H.S. (2016). AMPK phosphorylates desnutrin/ATGL and hormone-sensitive lipase to regulate lipolysis and fatty acid oxidation within adipose tissue. Mol. Cell Biol. *36*, 1961–1976.

56. Serrano, A.L., Baeza-Raja, B., Perdiguero, E., Jardí, M., and Muñoz-Cánoves, P. (2008). Interleukin-6 is an essential regulator of satellite cell-mediated skeletal muscle hypertrophy. Cell Metabol. *7*, 33–44.

57. Engelbrechtsen, L., Lundgren, J., Wewer Albrechtsen, N.J., Mahendran, Y., Iepsen, E.W., Finocchietto, P., Jonsson, A.E., Madsbad, S., Holst, J.J., Vestergaard, H., et al. (2017). Treatment with liraglutide may improve markers of CVD reflected by reduced levels of apoB. Obes. Sci. Pract. *3*, 425–433.

58. Akawi, N., Checa, A., Antonopoulos, A.S., Akoumianakis, I., Daskalaki, E., Kotanidis, C.P., Kondo, H., Lee, K., Yesilyurt, D., Badi, I., et al. (2021). Fat-secreted ceramides regulate vascular redox state and influence outcomes in patients with cardiovascular disease. J. Am. Coll. Cardiol. *77*, 2494–2513.

59. Lundgren, J.R., Janus, C., Jensen, S.B.K., Juhl, C.R., Olsen, L.M., Christensen, R.M., Svane, M.S., Bandholm, T., Bojsen-Møller, K.N., Blond, M.B., et al. (2021). Healthy weight loss maintenance with exercise, liraglutide, or both combined. N. Engl. J. Med. *384*, 1719–1730.

60. Ogata, A., Morishima, A., Hirano, T., Hishitani, Y., Hagihara, K., Shima, Y., Narazaki, M., and Tanaka, T. (2011). Improvement of HbA1c during treatment with humanised anti-interleukin 6 receptor antibody, tocilizumab. Ann. Rheum. Dis. *70*, 1164–1165.

61. Cuttler, A.S., LeClair, R.J., Stohn, J.P., Wang, Q., Sorenson, C.M., Liaw, L., and Lindner, V. (2011). Characterization of Pdgfrb-Cre transgenic mice reveals reduction of ROSA26 reporter activity in remodeling arteries. Genesis *49*, 673–680.

62. Gao, Z., Daquinag, A.C., Fussell, C., Zhao, Z., Dai, Y., Rivera, A., Snyder, B.E., Eckel-Mahan, K.L., and Kolonin, M.G. (2020). Age-associated telomere attrition in adipocyte progenitors predisposes to metabolic disease. Nat. Metab. *2*, 1482–1497.

63. Gao, Z., Daquinag, A.C., Fussell, C., Djehal, A., Désaubry, L., and Kolonin, M.G. (2021). Prohibitin inactivation in adipocytes results in reduced lipid metabolism and adaptive thermogenesis impairment. Diabetes *70*, 2204–2212.

STAR★METHODS

KEY RESOURCES TABLE

REAGENT or RESOURCE	SOURCE	IDENTIFIER
Antibodies		
Anti-UCP1	Alpha Diagnostic	Cat. # UCP-11A
Anti-Perilipin	Abcam	Cat. # ab61682
Anti-PDGFRβ	Abcam	Cat. # ab32570
Anti-IL-6R	R&D Systems	Cat. # AF1830
Anti-beta-actin	Abcam	Cat. # ab8224
Anti-pAMPK	Cell Signaling	Cat. # 2535
Anti-STAT3	Cell Signaling	Cat. # 9139
Anti-pSTAT3	Cell Signaling	Cat. # 9145
Anti-UCP1	Sigma	Cat. # U6382
IL-6 antibody BF09	R&D Systems	Cat. # AB-406-NA,
Donkey Alexa 488-IgG	Jackson ImmunoResearch	Cat. # A11055
Donkey Alexa Cy3-IgG	Jackson ImmunoResearch	Cat. # 711-166-152
Biological samples		
Patient blood samples	Hamidi et al.[26]	N/A
Chemicals, peptides, and recombinant proteins		
Rodent 58 kcal% (fat) diet	Research Diets	Cat. # D12331
Liraglutide	AdipoGen Life Sciences	Cat. # AG-CP3-0034-M005
Histopaque 1077	Sigma	Cat. # 10771
Human IL-6	R&D Systems	Cat. # 206-IL-010/CF
Mouse IL-6	R&D Systems	Cat. # 406-ML/CF
Trizol	Life Technologies	Cat. # 15596018
Hoechst 33258	Invitrogen	Cat. # H3569
Insulin	Sigma	Cat. # I9278
IBMX	Sigma	Cat. # I7018
Dexamethasone	Sigma	Cat. # D4902
3,3′,5-Triiodo-L-thyronine	Sigma	Cat. # T2877
Rosiiglitazone	Sigma	Cat. # R2408
Critical commercial assays		
IL-6 ELISA kit	R&D Systems	Cat. # 501030
NEFA kit	Fujifilm Wako Diagnostics	Cat. # NEFA-HR(2)
cDNA Reverse Transcription Kit	Applied Biosystems	Cat. # 4368814
Q-PCR Master Mix	Gendepot	Cat. # Q5600-005
Experimental models: Cell lines		
Primary mouse cells	This study	N/A
Experimental models: Organisms/strains		
C57BL/6	Jackson Laboratories	Cat. # 000664
IL-6ra^{fl}	Jackson Laboratories	Cat. # 012944
Pdgfrb-Cre	Jackson Laboratories	Cuttler et al.[61]
Oligonucleotides		
Ucp1 forward	Integrated DNA Technologies	5′-TCTCAGCCGGCTTAATGACTG-3′
Ucp1 reverse	Integrated DNA Technologies	5′-GGCTTGCATTCTGACCTTCAC-3′;
SOCS3 forward	Integrated DNA Technologies	5′-GGACCAAGAACCTACGCATCCA-3′
SOCS3 reverse	Integrated DNA Technologies	5′-CACCAGCTTGAGTACACAGTCG-3′

(*Continued on next page*)

Continued

REAGENT or RESOURCE	SOURCE	IDENTIFIER
ADAM10 forward	Integrated DNA Technologies	5′-ATGGTGTTGCCGACAGTGTTA-3′
ADAM10 reverse	Integrated DNA Technologies	5′-GTTTGGCACGCTGGTGTTTTT-3′
18 S RNA forward	Integrated DNA Technologies	5′-AAGTCCCTGCCCTTTGTACACA-3′
18 S RNA reverse	Integrated DNA Technologies	5′-GATCCGAGGGCCTCACTAAAC-3′

RESOURCE AVAILABILITY

Lead contact

Further information and requests for resources and reagents should be directed to and will be fulfilled by the lead contact, Mikhail Kolonin (Mikhail.G.Kolonin@uth.tmc.edu).

Materials availability

Tissues from designed mouse strains are available from the lead contact, Mikhail Kolonin (Mikhail.G.Kolonin@uth.tmc.edu), with a material transfer agreement through UTHealth.

Data and code availability

- Data reported in this paper will be shared by the lead contact upon request.
- This paper does not report custom code,
- Any additional information required to reanalyze the data reported in this work paper is available from the lead contact upon request.

EXPERIMENTAL MODEL AND SUBJECT DETAILS

Human subjects

The protocol was approved by the Committee for the Protection of Human Subjects at the University of Texas Health Science Center at Houston. Written informed consent was provided by all human subjects prior to participation. The design of the prospective randomized crossover placebo-controlled double-blinded trial was reported previously.[26] Eligible subjects were men and women, ages 30 to 70 years, with prediabetes. Prediabetes was defined as impaired fasting glucose (100–125 mg/dL), impaired glucose tolerance (2-h postprandial glucose of 140–199 mg/dL after 75 g oral glucose challenge), and/or a hemoglobin A1C ranging from 5.7% to 6.4%. Qualified subjects had a BMI of 30–35 mg/kg^2 ($\pm$1 mg/kg^2), with stable body weight (i.e., no change in weight greater or less than 5 pounds) for the prior three months. Women of childbearing age agreed to a nonhormonal pregnancy prevention method (barrier methods, abstinence, or prior surgical sterilization). On screening, the following laboratory values were required: hematocrit $\geq$34%, serum creatinine <1.5 mg/dl in men and 1.4 mg/dl in women, AST (SGOT) < 2.5 times upper limit of normal (ULN), ALT (SGPT) < 2.5 times ULN, and alkaline phosphatase< 2.5 times ULN. Statins, ACE inhibitors, and angiotensin-receptor blockers were allowable at stable doses for at least three months prior to study enrollment, and throughout the duration of the study. No subjects received non-statin lipid-lowering medications, metformin, DPP-IV inhibitors, GLP1RAs, sodium-glucose cotransporter-2 (SGLT-2) inhibitors, thiazolidinediones, insulin, sulfonylureas, corticosteroids, hormone replacement therapy, nor immunosuppressive therapy for at least three months prior to the start of the study. NSAIDs and antioxidant vitamins were discontinued one week prior to study initiation and for the duration of the study. Exclusions were significant cardiac, hepatic, or renal disease, current tobacco use, active malignancy, or diabetes mellitus, prior history of pancreatitis, prior history of medullary thyroid cancer, and prior history of multiple endocrine neoplasia 2 (MEN2). Pregnant and breastfeeding women were excluded.

Animals

The protocol was approved by Institutional Animal Care and Use Committee at The University of Texas Health Science Center at Houston. C57BL/6, and IL-6R$^{flox/flox}$ (Stock 012944) mice were from Jackson Laboratories. *Pdgfrb-Cre* strain was described previously.[35,61] Mice were housed in the animal facility with a 12-h light/dark cycle and constant temperature (22–24°C). For DIO induction, mice were fed 58 kcal% (fat) diet (Research Diets, D12331). Body composition was measured by EchoMRI-100 T (Echo Medical Systems). Liraglutide (AdipoGen Life Sciences AG-CP3-0034-M005) was injected intraperitoneally (i.p.) five days/week. The blocking IL-6 antibody BF09 (AB-406-NA, R7D Systems) was injected i.p. three days/week. GTT was done one day before the last injection and CTT - two days after the last injection. For GTT, glucose (2 g/kg body weight) was injected i.p. into overnight-fasted mice and then blood glucose concentration was measured with a glucometer (One Touch Ultra). For CTT, core body temperature was determined in the rectum 2.5 cm deep using a MicroTherma 2K High Precision Type K Thermocouple Meter (THS-221-092, ThermoWorks) with

RET-3 probe (Braintree Scientific) upon placing mice at 4°C. Indirect calorimetry studies were performed with OXYMAX (Columbus Instruments) Comprehensive Lab Animal Monitoring System (CLAMS) as described.[35,62,63]

METHOD DETAILS

Cell analysis

For PBMC isolation, blood sample from a healthy donor was collected in Na-EDTA tubes and centrifuged at 450 g for 10 min at 20°C. Plasma layer was removed. The resultant cell suspension was layered on Histopaque 1077 (Sigma). Phospho-buffered solution (PBS) was added and tubes were centrifuged at 800 g for 15 min at 20°C. Supernatant was aspirated and discarded, and the interphase layer was transferred to a 50 cc conical tube and filled with PBS for a total volume of 50 cc. Solution was centrifuged at 1300 RPM for 10 min at 20°C. New supernatant was discarded and resulting pellet was plated in culture to select monocytes based on adherence. Human primary ASC/preadipocytes, isolated from SAT previously, were cultured as described.[35,62] Human IL-6 (206-IL-010/CF) and mouse IL-6 (406-ML/CF) were from R&D Systems. Mouse immortalized brown pre-adipocytes were induced for adipogenesis in 50 nM insulin/0.5 mM IBMX, 1 μM dexamethasone, 1 nM 3,5,3′-Triiodothyronine (T3) and 5 μM rosiglitazone as described.[35]

Tissue analysis

IL-6 concentration in plasma and medium was determined by an ELISA kit #501030 (R&D Systems). Plasma FFA concentration was determined by an enzymatic colorimetric quantification method (Fujifilm Wako Diagnostics). Plasma insulin was determined by chemiluminescent immunoassay (Beckman Coulter). A hexokinase assay was used to measure plasma glucose (Beckman Coulter). Paraformaldehyde-fixed cells and formalin-fixed paraffin-embedded tissue sections were analyzed by IF upon antigen retrieval as described.[35,62,63] Upon blocking, the following primary antibodies diluted in phosphate-buffered saline (PBS) with 0.05% Tween 20 were used (4°C, 12 h): Anti-UCP1 from Alpha Diagnostic, Cat. # UCP-11A (1:400); anti-Perilipin from Abcam, ab61682 (1:200); Anti-PDGFRβ from Abcam, ab32570 (1:50); Anti-IL-6R from R&D Systems, AF1830 (1:50). Secondary antibodies (RT, 1 h) were Donkey Alexa 488-conjugated (1:200) and Cy3-conjugated (1:300) IgG from Jackson ImmunoResearch. Nuclei were stained with Hoechst 33258 (Invitrogen, H3569). IF images were acquired with Carl Zeiss upright Apotome Axio Imager Z1/ZEN2 Core Imaging software. Amira 5.4 software (VSG) was used for data capture and analysis. Image J analysis software was used to quantify data.

Quantitative real-time RT-PCR

Total RNA was extracted using Trizol (Life Technologies, 15596018). Complementary DNAs were generated using the High-Capacity cDNA Reverse Transcription Kit (Applied Biosystems, 4368814). PCR reactions were performed on a CFX96 Real-Time System C1000 Touch thermal cycler (Bio-Rad) using Q-PCR Master Mix (Gendepot, Q5600-005). Expression of mouse *Ucp1* was normalized to *18 S* RNA. Primers were as follows: *Ucp1*, 5′-TCTCAGCCGGCTTAATGACTG-3′ and 5′-GGCTTGCATTCTGACCTTCAC-3′; *SOCS3*: 5′-GGACCAAGAACCTACGCATCCA-3′ and 5′-CACCAGCTTGAGTACACAGTCG-3′; *ADAM10*: 5′-ATGGTGTTGCCGA CAGTGTTA-3′ and 5′-GTTTGGCACGCTGGTGTTTTT-3′; and *18 S RNA*, 5′-AAGTCCCTGCCCTTTGTACACA-3′ and 5′-GATCC GAGGGCCTCACTAAAC-3′.

Western blotting

Whole-cell lysates were prepared in RIPA buffer and analyzed as described previously.[62,63] AT lysates were separated by SDS-PAGE and subsequently analyzed by immunoblotting. The following antibodies were used: anti-STAT3 (Cell Signaling, 124H6), anti-pSTAT3 (Cell Signaling, 9145); anti-UCP1 (Sigma, U6382; 1:5000); anti-pAMPK (Cell Signaling, 2535) and anti-β-actin (Abcam, ab8224; 1:5000). The signal was detected using the Odyssey DLx imaging system (LI-COR) and quantified with Image J analysis software.

QUANTIFICATION AND STATISTICAL ANALYSIS

For human studies, with a two-sided alpha of 0.05 and a beta of 0.20, a paired Student t-test was used. Pairwise group comparison was performed at each measurement time, adjusted for multiple testing by Tukey's method. Outcomes for each drug at each subsequent measurement times were compared with their corresponding values at baseline and adjusted for multiple testing as well. All analyses were performed in SAS 9.4 software and Stata/IC 14.1 (StataCorp). For mouse and cell culture data, statistical analyses were performed with GraphPad Prism 6 software. Student's unpaired t-test and one-way ANOVA with Šídák's post-hoc test (for multi-group comparisons) were performed unless otherwise indicated. $p < 0.05$ was considered significant. Experimental results are shown as mean ± SEM.

ADDITIONAL RESOURCES

Results from the prospective randomized crossover placebo-controlled double-blinded trial https://clinicaltrials.gov/ct2/show/NCT02104739 have been reported.[26]

Cell Reports Medicine, Volume *3*

Supplemental information

Anti-diabetic effects of GLP1 analogs are mediated by thermogenic interleukin-6 signaling in adipocytes

Absalon D. Gutierrez, Zhanguo Gao, Vala Hamidi, Liang Zhu, Karla Bermudez Saint Andre, Kayla Riggs, Monika Ruscheinsky, Hongyu Wang, Yongmei Yu, Charles Miller III, Hernan Vasquez, Heinrich Taegtmeyer, and Mikhail G. Kolonin

n	16
Ethnicity (Caucasian/Black/Hispanic/Pacific Islander)	3/8/4/1
Gender (M/F)	9/7
Age (years)	50 ± 8
Weight (kg)	94.3 ± 11.7
BMI (kg/m^2)	32.5 ± 1.8
SBP (mm Hg)	136 ± 23
DBP (mm Hg)	79 ± 11
Fasting glucose (mg/dL)	93 ± 9
Fasting insulin (mIU/L)	8.2 ± 6.2
HOMA-IR	1.98 ± 1.85
Hemoglobin A1c (%)	5.96 ± 0.23
Triglycerides (mg/dL)	122 ± 55
Total cholesterol (mg/dL)	198 ± 44
HDL cholesterol (mg/dL)	54 ± 10
LDL cholesterol (mg/dL)	120 ± 43
AST (units/L)	21 ± 7
ALT (units/L)	22 ± 12
Creatinine (mg/dL)	0.98 ± 0.26
Hemoglobin (g/dL)	13.8 ± 1.0
Platelets ($x10^9/L$)	233 ± 54

Table S1 - **Baseline Clinical Characteristics of Study Participants.**

Related to Figure 1

Data are means ± SD.

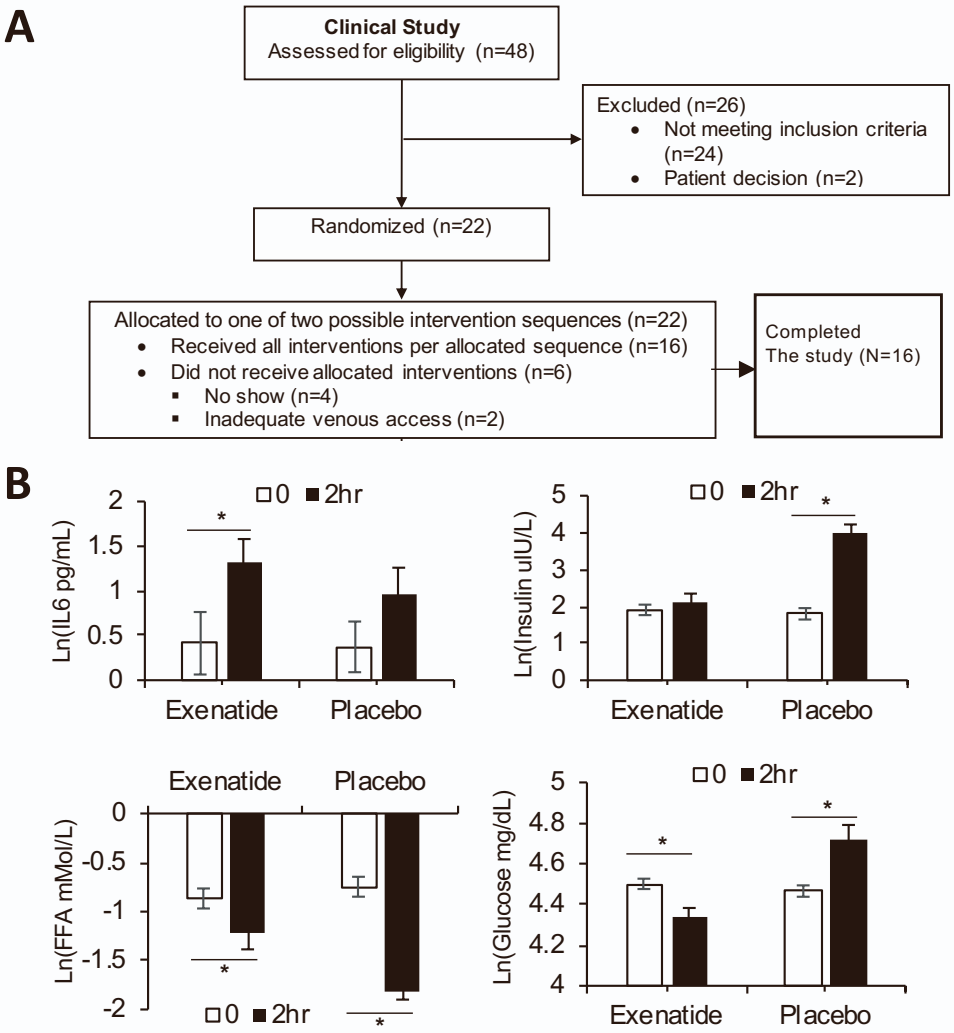

Figure S1 Clinical study. Related to Figure 1.
(A) Study design. The study was a single center, randomized, crossover, double-blinded, placebo-controlled trial. Simple randomization (for study drug order in each participant) was achieved via a computer-generated algorithm. Allocation concealment was maintained by independent study pharmacists. Blinding of intervention sequence (to investigators and subjects) was achieved through the use of an identical-appearing placebo (i.e., normal saline served as the placebo for exenatide). All analyses were conducted as intention-to-treat. Potential subjects participated in a screening visit, where a complete history and physical examination was performed, followed by laboratory testing. Qualified subjects completed two separate, daylong outpatient studies at the Clinical Research Unit (CRU). On each study day, subjects were given a single dose of exenatide 10 mcg by subcutaneous (sc) injection or the same volume of placebo by sc injection. Each study was performed at least 10 days apart to ensure adequate washout of study medication. The study day began at 8:00 AM after an overnight fast and avoidance of alcohol and excessive exercise for 24 hr. An intravenous catheter was placed in a stable vein in an upper extremity. Baseline blood draw was collected a few minutes before the scheduled 11:00 AM meal. Then study medication was given immediately. Then at 11:00 AM subject began eating a timed standardized test meal which consisted of a hamburger, French fries, small apple pies, and diet soda (1550 kcal; 700 kcal from fat; 60% carbohydrate, 30% fat, and 10% protein). The subject was given up to 30 minutes to complete the meal. Venous blood samples were collected again 2 hours later. These procedures were repeated for the second study arm. This study design is similar to our previously described protocol (Hamidi et al., 2020).
(B) Plots of natural log-transformed Figure 1A data, which are not normally distributed.
*$p<0.05$, Student's t-test.

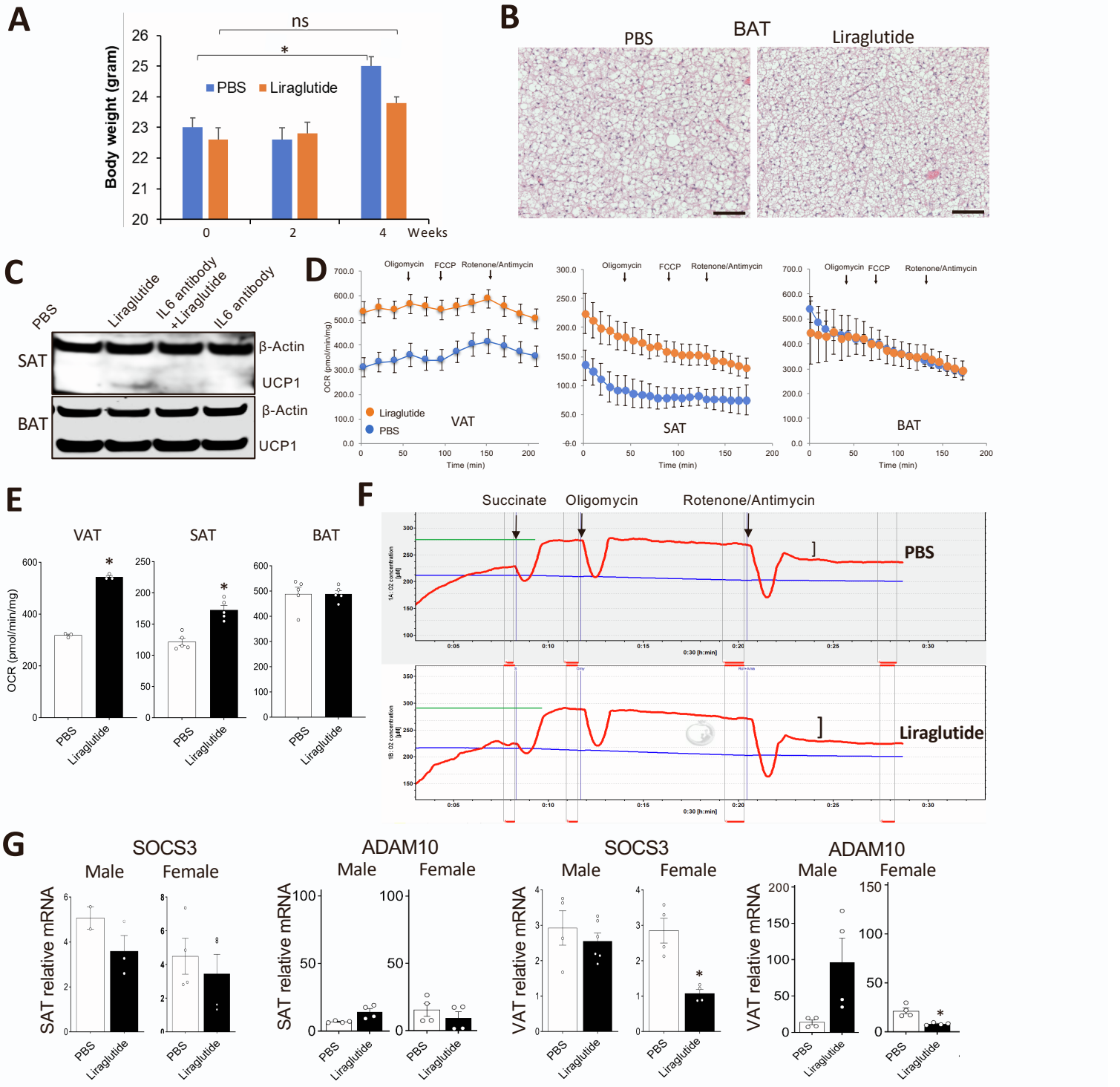

Figure S2 Liraglutide induces IL6 signaling and adipocyte browning in mice. Related to Figure 2.

(A) EchoMRI analysis of HFD-fed overweight C57BL/6 males after 2 and 4 weeks of liraglutide, treatment shows reduced body mass gain in liraglutide-treated mice. n=5. ns: non-significant; *p<0.05, Student's t-test.

(B) BAT sections from mice in (A) at week 4 stained with H&E. Scale bar: 50 µm.

(C) Analysis of mice in Fig. 3 by immunoblotting with the indicated antibodies shows liraglutide-induced UCP1 expression in SAT, but not in BAT. Actin: loading control.

(D) Increased mitochondrial Respiration in VAT, SAT, but not in BAT, of mice treated with liraglutide in a Seahorse Mito Stress Assay performed with XFe24 (Agilent Technologies). n=5 to 10 wells.

(E) Average basal oxygen consumption rate (OCR) calculated from Seahorse data in (D). *p<0.05, Student's t-test.

(F) Increased respiration in SAT of mice treated with liraglutide, compared with control mice, measured by Oroboros Oxygraph O2k Respirometer. Red: O_2 flux. Green : maximal respiration upon succinate treatment.
]: uncoupled respiration (post-Oligomycin value minus post-Rotenone/Antimycin value). Performed once.

(G) C57BL/6 males were injected with a single s.c. dose of liraglutide (0.2mg/kg BW). Analysis of SAT and VAT by RT-PCR after 24 hr shows a trend for a reduction in relative SOCS3 and ADAM10 expression (normalized to 18SRNA). *p<0.05, Student's t-test.

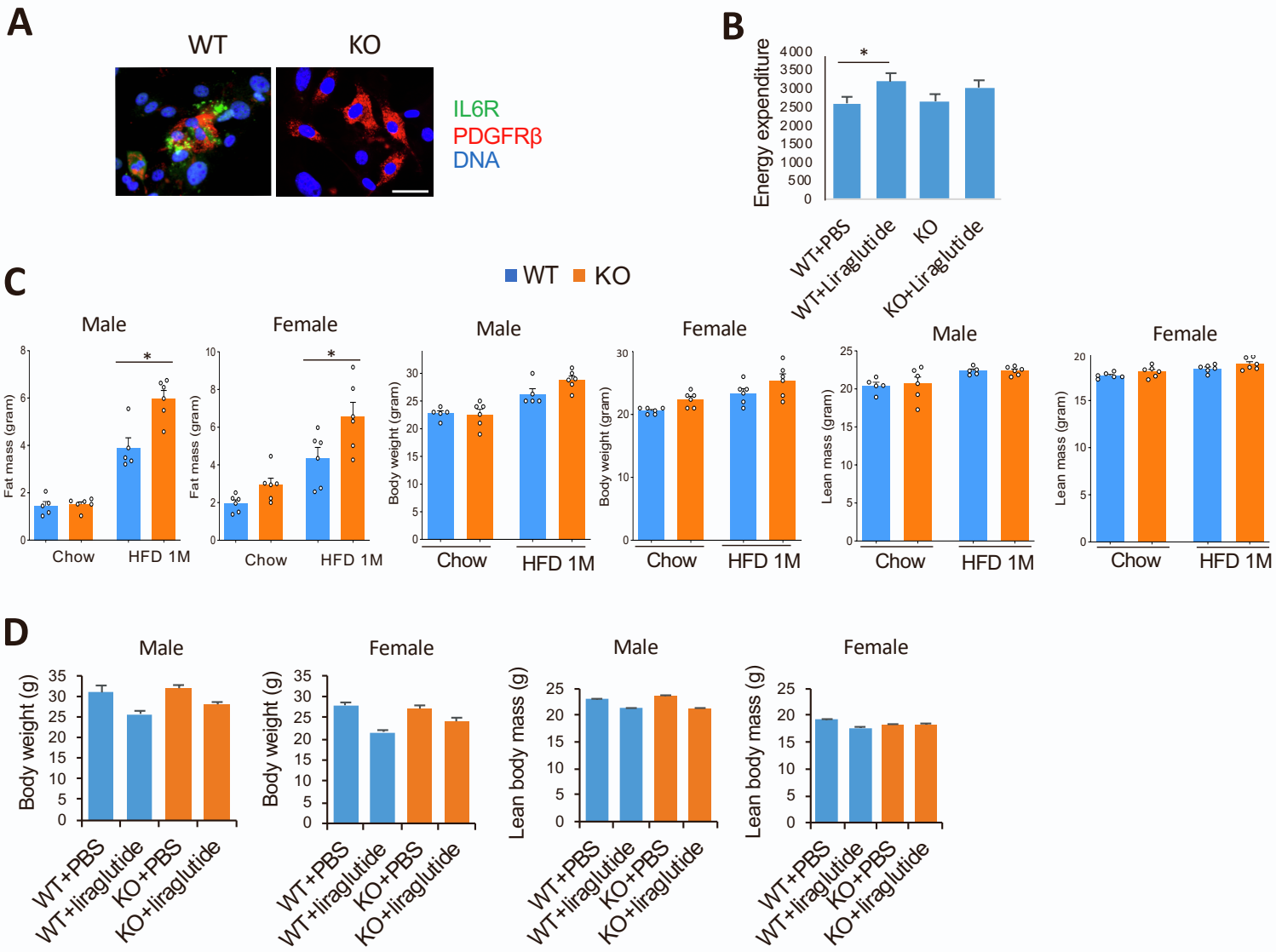

Figure S3. IL6R KO in adipocyte progenitors negates thermogenic effect of liraglutide. Related to Figure 4.
(A) SVF from AT of WT and Pdgfrb-Cre; IL6R$^{fl/fl}$ (KO) mice subjected to IF. Note that IL6R protein expression (green) is lost in PDGFRβ+ ASCs of KO mice. Scale bar: 50 µm.
(B) Energy expenditure in C57BL/6 and IL6R KO males and females after 4 weeks of liraglutide, treatment measured based on Oxygen consumption (VO_2) by indirect calorimetry during the night. Note that the liraglutide-induced increase observed in WT mice is not observed in KO mice. n=3. *p<0.05, Student's t-test.
(C) EchoMRI analysis of C57BL/6 and IL6R KO males after feeding with chow or HFD for 1 month.
(D) EchoMRI analysis of mice in (B). After 4 weeks of liraglutide, treatment (0.2 mg/kg s.c. 20 metronomic injections) the trends for lean and total body mass are similar in WT and KO mice.

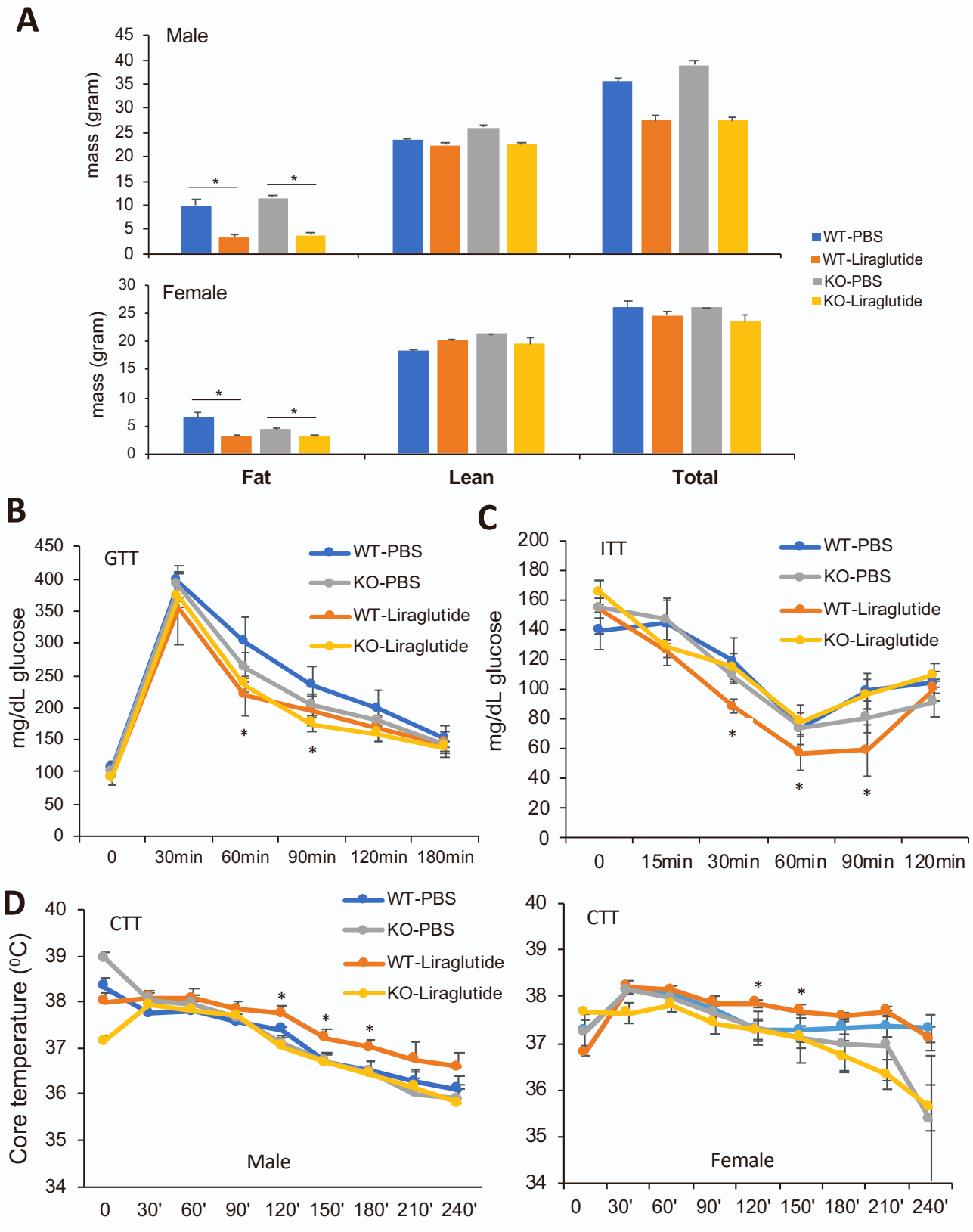

Figure S4. IL6R KO in mature adipocytes negates thermogenic effect of liraglutide. . Related to Figure 4. Adiponectin-Cre;IL6Rafl/fl (KO) and control L6Rafl/fl (WT) progeny were compared.
(A) EchoMRI analysis of HFD-fed overweight C57BL/6 and KO males and females after 4 weeks of liraglutide, treatment (0.2 mg/kg i.p. 20 metronomic injections). Note the reduction of fat mass in both WT and KO liraglutide-treated males and females.
(B) Analysis of mice in (A) at week 4 by glucose tolerance test in males.
(C) Analysis of mice in (A) at week 4 by insulin tolerance test (ITT) in males.
(D) Analysis of mice in (A) at week 4 by cold tolerance test in males and females.
(A-D): n=5. *p<0.05 (1-way ANOVA) for WT PBS vs WT-Liraglutide comparison. Not significant for KO mice.